

A Model of Mesons

R Wayte

29 Audley Way, Ascot, Berkshire, SL5 8EE, England, UK.

e-mail: rwayte@googlemail.com

Research article. Submitted to vixra.org 19 September 2011

Abstract: Detailed models of mesons have been derived in terms of real structured particles, in order to replace the formless quark/anti-quark singularities of standard QCD theory. Pion design is related to the muonic mass, and a Yukawa potential is calculated for the hadronic field. A charged pion is produced by adding a heavy-electron or positron in a tight orbit around the neutral core. Other mesons are found to be ordered assemblies of pionic-size masses, travelling in bound epicyclical orbits, with real intrinsic spin and angular momentum. These orbit dimensions are related to the mean lifetimes of the mesons through action integrals. Decay products resemble parts of their parent mesons, as expected for a relaxation process with traceability of particles.

Key words: meson composite models

PACS Codes: 12.39.Pn, 12.60.Rc, 14.40.Be, 14.40.Df

1 Introduction

According to standard QCD theory, mesons have overall finite dimensions yet consist of quark plus anti-quark singularities of infinite mass density. This is not realistic and is of limited value in explaining the meson variations from type to type. Of course, quantum theory is essential for describing *interactions between* particles, yet it tells us little about particle structure, and there remains the need to elevate quantum theory above mathematical inspiration or fantasy.

Comprehension of this analysis requires some unique concepts developed previously for fermion models; see Wayte, Papers 1, 2, 3. Those models described an *isolated* proton, electron or muon and were very successful at explaining the Yukawa potential, the reality of spin and anomalous magnetic moment, and particle creation mechanisms. On the other hand, the Standard Model of particle *interactions* has been very successful at accounting for data from high energy collision experiments. Consequently, the conceptual differences between these models can be explained if particles in collisions reveal behaviour not immediately apparent in static models. To link these models, the constituents of baryons and mesons need to *behave* like up, down and strange quarks when in high energy collisions. It will be shown in Appendix A how this happens.

When we consider that high energy collision experiments are theoretically capable of producing a continuum of meson types, it must be significant that so few types are somehow chosen to exist. Mesons will be described as real understandable mechanisms with variability in their substructure for the different types. In collisions and decay processes, historic traceability of products is considered to be very important as a guide to design. Spin and angular momentum are always real structured quantities. As for fermions, particle mass is simply localised energy travelling at the velocity of light in bound orbits, so the Higgs postulate is unnecessary. This bound energy has helicity which determines by whether the particle is matter or anti-matter. A fundamental particle satisfies the Dirac equation but any concept of negative mass-energy or time-reversal is excluded. Real particles are covered by their wavefunction:

$$\Psi = Ae^{\pm i(Et - px)/\hbar}, \quad (1.0)$$

where $+i$ means right-handed helicity and $-i$ means left-handed helicity of a circularly polarised wavefunction; and E , t are real positive quantities only.

In this static meson model there are indeed two major pieces, but they do not look or behave like QCD quarks, so they will be called *quion* q^+ and *anti-quion* q^- according to their charge sign. These orbit the origin and can produce real spin angular momentum, depending on their orientation and the orbit radius. Often, there is also an extra complex particle located at the origin, which increases the mass and adds variety to meson behaviour. We will start with the pion model as the basic design, and then extrapolate to cover other mesons.

The lifetime of a free meson must depend upon its particular internal design. This inference is based upon analogy with other physical systems; for example when a charged capacitor C is connected to a resistor R, the discharge time constant is determined by the hardware involved (CxR). Several separate batches of a given meson type will decay so as to converge upon the same characteristic lifetime; therefore the same exact mechanism must exist in all batches. The probability that a single meson will decay in any given time increment is a constant, so no ageing occurs. This implies that the smooth-running mechanism is perfect but subject to spontaneous quantum fluctuations of the internal fields which can disturb it catastrophically. Different types of mesons have characteristic lifetimes and mechanisms but there are some common features.

The way that the meson's mean lifetime τ and decay width Γ cooperate during its creation in a collision process is interesting. Given:

$$\Gamma\tau \approx \hbar, \quad (1.1)$$

the real value of Γ must be established in the short creation period, whereas τ and the decay probability appear realised *after the creation is completed*, over a much longer period in some cases. This contrasts with an atomic emission-line in which the scatter in energy depends upon the lifetime of the excited state *before emission*. Furthermore, the Heisenberg uncertainty principle is written:

$$\Delta E\Delta t \approx \hbar \quad \text{or} \quad \Delta x\Delta p \approx \hbar, \quad (1.2)$$

where Δt implies incremental uncertainty in a larger macroscopic value of t ; but τ in Eq.(1.1) is the macroscopic value. Effectively, τ is established during the creation stage as a coherence period of the controlling guidewave, (see Paper 1, Section 10.3). The decay probability wavefunction follows as a consequence of this.

Section 2 will now concentrate on the detailed pion design. Section 3 will cover the well-observed unflavoured mesons and Section 4 the remaining unflavoured mesons. Section 5 describes the designs of strange mesons. Section 6 is the general conclusion. Appendix A explains the compatibility of these designs with the Standard Model for protons, neutrons and mesons.

All particle data have been taken from the Particle Data Group listing at <http://pdg.lbl.gov>.

2 Pions

$$\begin{aligned} \pi^0(135) : m &= 134.9766 \text{MeV}/c^2, I^G(J^{PC}) = 1^-(0^{-+}) \\ \pi^\pm(140) : m &= 139.57018 \text{MeV}/c^2, I^G(J^P) = 1^-(0^-) \end{aligned}$$

In QCD theory, a pion is thought to consist simply of a quark and anti-quark with net charge determined by the type of quarks. The pion *effective* charge radius has been measured at around 0.65fm, see Amendolia et al. (1986) and Eschrich et al. (2001).

Our pion model is illustrated in Figure 2.1, wherein a quion q^+ and anti-quion q^- , each consisting of two smaller pearls, orbit the centre at radius $r_{0\pi}$ and velocity c to constitute a π^0 neutral pion. These may then be orbited by a heavy-positron to make a π^+ (classed as matter), or a heavy-electron to make a π^- (anti-matter). Analogous to the proton and antiproton, the quion and anti-quion emit a radial pionic-type field, in addition to possessing their own native electromagnetic charge, plus a gluonic strong-field running around their own circumferences. Overall angular momentum of the pion is zero because the pair rotate about their own axes, counter to their orbital motion, that is:

$$m_q c' r_q = m_q c r_{0\pi} \quad , \quad (2.1)$$

where $[c' = c(\pi/2)]$, $[r_q = r_{0\pi}(2/\pi)]$, and $[r_{0\pi} = 2e^2 / m_{\pi_0} c^2]$.

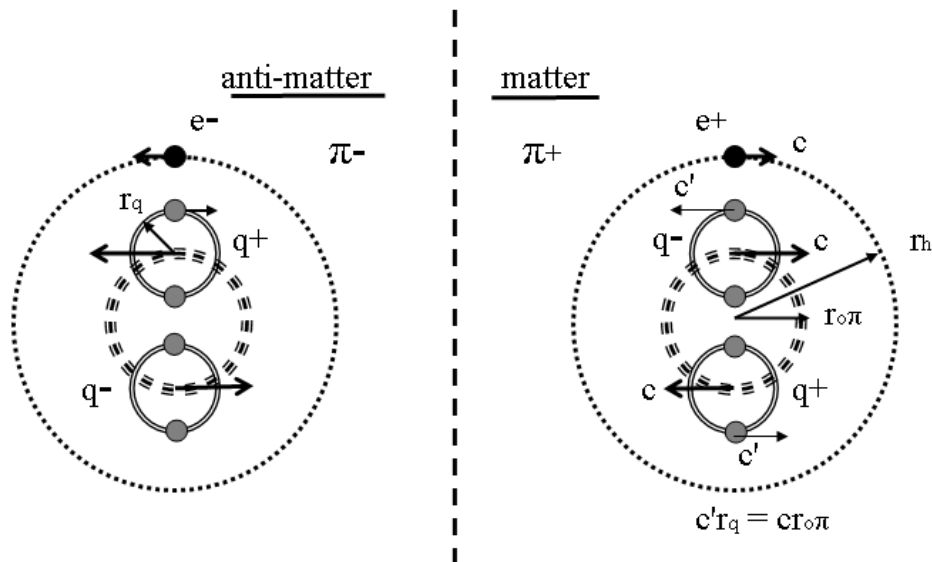


Fig.(2.1) Pion component parts for matter π^+ and anti-matter π^-

2.1 Yukawa potential

The quion /anti-quion pair is proposed to emit an attractive nuclear-type hadronic field similar to the proton; wherein the ‘field-mesons’ have reduced effective masses [$m_{\pi'} = m_{\pi_0}(h'/h)$ with $h' \ll h$] in order to produce a smooth copious field. Published QCD calculations will here be considered unrealistic if the exchange field particles are as massive as the source particle, see for example Gashi et al. (2001). Nevertheless, the calculations may still be useful if aspects like field *range* can be re-expressed in terms of the mass $m_{\pi'}$.

The metric tensor component for the field is proposed to be analogous to the proton field, (see Paper 1, Eq.(3.4)):

$$\gamma = \left[1 - \left(\frac{r_{0\pi}}{r} \right) \exp - \left(\frac{r - r_{0\pi}}{r_{\pi}} \right) \right]^{1/2}, \quad (2.2)$$

where ($r_{\pi} = \hbar/m_{\pi_0}c = 1.462\text{fm}$) is the range factor, and ($r_{0\pi} = 2e^2/m_{\pi_0}c^2 = 2r_{\pi}/137$) is *double* the pion classical radius because of the quion /anti-quion pair; compare this with positronium. The corresponding empirical potential is given by:

$$V_c = (\gamma - 1) \left(\frac{m_{\pi_0}c^2}{a_{\chi\pi}} \right), \quad (2.3)$$

where $a_{\chi\pi}$ represents the hadronic charge for pions, to be determined shortly. Then, from Eqs.(3.8) (3.9) in Paper 1, the hadronic coupling constant for (π - π) is definable as:

$$\chi_{\pi} = \left[\left(\frac{m_{\pi_0} c^2 r_{0\pi}}{2} \right) \exp\left(\frac{r_{0\pi}}{r_{\pi}} \right) \right] / \hbar c \approx \left(\frac{(1 + 2/137)}{137} \right). \quad (2.4a)$$

This ‘mesonic-field’ is independent of any electromagnetic positive or negative charge which orbits the hadronic pair. For pion-nucleon interactions it is probable that the coupling constant will be of the order:

$$\chi_{\pi N} = (\chi_N \chi_{\pi})^{1/2} \approx (9/137) \approx 0.065, \quad (2.4b)$$

where the nucleon-nucleon coupling constant is ($\chi_N \approx 1/\sqrt{3}$) in Paper 1.

Analogous to the proton derivation, hard core repulsion will be attributed to rapid spinning of the quion/anti-quion field source which modulates the local field and causes it to become repulsive. Here, the source frequency is ($c/2\pi r_{0\pi}$) compared with the Compton frequency of field-mesons ($c/2\pi r_{\pi}$); that is, (137/2) times greater. Therefore, analogous to Eq.(4.1) of Paper 1, the full hard core metric tensor component becomes:

$$\gamma_{hc} = \left\{ 1 - \left(\frac{r_{0\pi}}{r} \right) \left[1 - \left(\frac{r_{\pi}}{r_{0\pi}} \right) \left(\frac{r_{0\pi}}{r} \right) \exp\left(-\frac{r - r_{0\pi}}{r_{0\pi}} \right) \right] \exp\left(-\frac{r - r_{0\pi}}{r_{\pi}} \right) \right\}^{1/2}. \quad (2.5)$$

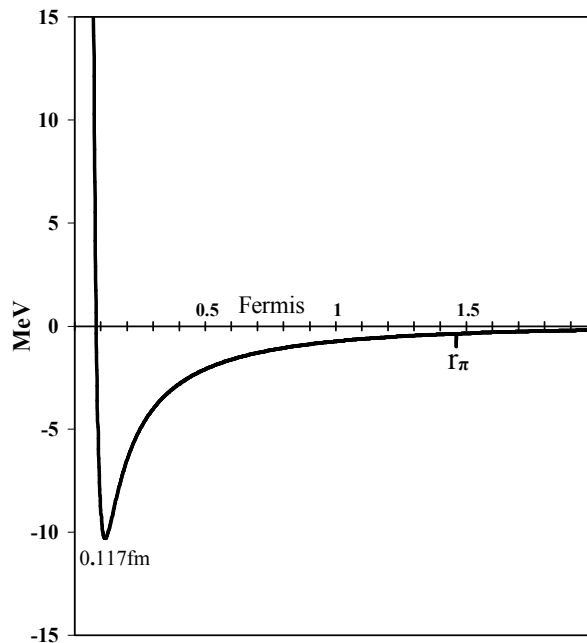


Fig.(2.2) Hadronic potential energy function for the pion.

The empirical overall pion potential is given by:

$$V_{\text{hc}} = (\gamma_{\text{hc}} - 1) \left(\frac{m_{\pi_0} c^2}{a_{\chi\pi}} \right), \quad (2.6)$$

where $[a_{\chi\pi} = (\chi\pi\hbar c)^{1/2}]$. This potential energy ($a_{\chi\pi} V_{\text{hc}}$) as a function of radius is illustrated in Figure 2.2.

2.2 Pion mass

The quion /anti-quion masses may be related to electronic mass or to muonic mass as was found for the pearls in a proton:

$$m_{\pi_0} = 2m_{\text{q}} = 264.1426m_{\text{e}} = 134.9766 \pm 0.0006 \text{ MeV}/c^2, \quad (2.7)$$

and given muon mass ($m_{\mu} = 105.658367 \text{ MeV}/c^2$) we have:

$$m_{\pi_0} = 2m_{\text{q}} \approx 2 \times \left\{ 2 \left(\frac{m_{\mu}}{3} \right) \left(1 - \frac{1}{24} \right) \right\}. \quad (2.8)$$

Here, we recall that a muonic mass could consist of 3 distinct packs of core-segments (Paper 3, Eq.(4.2)); consequently each quion pearl here takes the mass of one such pack ($m_{\mu}/3$), approximately. The small negative term in this equation will be taken to express overall mass decrement due to binding energy of the attractive field between pearls within the quion itself, plus the binding energy of the quion /anti-quion pair in the pion circumference.

Similar to the proton model, we shall further assume that:

$$\left(1 - \frac{1}{24} \right) \equiv \left(1 - \frac{r_{\ell}}{r_{\text{q}}} \right), \quad (2.9)$$

where the real quion radius is ($r_{\text{q}} = r_{\text{on}\pi}(2/\pi)$), and the pearl radius r_{ℓ} is thus:

$$r_{\ell} = \frac{r_{\text{q}}}{24} = \left(\frac{e^2}{m_{\text{q}} c^2} \right) \frac{(2/\pi)}{24}. \quad (2.10)$$

This implies that a pearl is dimensionally 24 times smaller than the quion, and that there were 24 original pearl-seed particles which subsequently condensed into 2 equal pearls of mass m_{ℓ} to minimise action /energy, analogous to the 3 pearls in a proton's trineon. It is thought probable that a pearl consists of 24 gluon-loops, like a proton pearl, but their constituent grains and mites are undefined.

The quion charge e was originally divided between the 24 pearl-seeds, thus:

$$\left(\frac{e}{m_q}\right) = \left(\frac{e/24}{m_{\ell s}}\right) = \left(\frac{e/2}{m_\ell}\right) \quad . \quad (2.11)$$

2.3 Charged pions

A charged pion is produced by adding a heavy-electron or positron to orbit the central quion /anti-quion pair. This increases the total mass, as was found for the neutron in Paper 1, viz:

$$\pi^\pm - \pi^0 = 4.5936 \pm 0.0005 \text{MeV} / c^2 = 8.9894 m_e = m_h \quad (2.12)$$

We shall assume that the mass increase is due solely to the orbiting heavy-electron (or positron), with its compressed dimensions. Thus, the classical radius of this heavy-electron is to be equal to the orbit size:

$$r_h = e^2 / m_h c^2 = 0.31347 \text{fm} . \quad (2.13)$$

At first sight this result appears arbitrary and does not explain why an electron should attach itself to the hadronic core at all. However, by referring to the neutron analysis, a proper physical explanation can be derived. The π^0 radius is given above as ($r_{0\pi} = 2e^2 / m_{\pi 0} c^2 = 0.0213365 \text{fm}$), consequently ($r_h = 14.692 r_{0\pi}$). Then this ratio of radii must govern a special relationship because the neutral π^0 and heavy-electron cooperate to produce a *more stable charged pion*,. Consequently, it is proposed that spiralling electromagnetic feeler guidewaves are emitted by the charged quion and anti-quion to communicate attractively and continuously with the heavy-electron (or positron). An action equation for these guidewaves will be based upon the following formula:

$$\ln(r_h / r_{0\pi}) = \ln 14.692 \approx \pi(e_n / \pi) \quad . \quad (2.14)$$

This may be differentiated and reduced to an electromagnetic action integral upon multiplying through by ($2e^2 / c = m_{\pi 0} c r_{0\pi}$):

$$2 \times \left(\frac{\pi}{e_n}\right) \times \int_{2\pi r_{0\pi}}^{2\pi r_h} \frac{\delta(e^2)}{z} dt \approx \int_0^{2\pi} \frac{\delta(m_{\pi 0})}{2} c r_{0\pi} d\theta . \quad (2.15)$$

where δ may be around h'/h , as used in Section 2.1. On the left is potential energy action for the feeler guidewave spiralling *out and back* from the quion and anti-quion,

with ($z = ct = 2\pi r$) and including a contribution from the gluon energy, through factor (π/e_n). On the right is kinetic energy action for the element of pion core material which constitutes the guidewave energy.

Finally, the manner in which the free electron (or positron) is compressed onto the π^0 core is interesting. Let the free electron spin-loop be first compressed down to electron core radius r_{oe} , then further to ($r_{he} = r_{oe}/2.843$), as was found for the neutron (see Paper 1). This is followed by compression by factor ($r_{he}/r_h = 3.1619$) to get to the final radius r_h . Then ($\ln(r_{he}/r_h) \approx \pi/e_n$) may be reduced to an action integral by differentiation and applying Eq.(2.13):

$$- \int_{2\pi r_{he}}^{2\pi r_h} \left(\frac{e^2}{z} \right) dt \approx \int_0^{2\pi} \frac{m_h}{2} c r_h \left(\frac{1}{e_n} \right) d\theta \quad . \quad (2.16)$$

On the left is action due to potential energy of the collapsing electron charge loop ($z = 2\pi r$), rotating at velocity c . The right side represents action of kinetic energy around the loop for a second harmonic material helix.

2.4 Pion mean lifetimes

It has been shown previously that the lifetime of a neutron or muon may be related to its internal period, by way of an action integral. Similarly, the pion lifetimes appear to be definite functions of internal periods, as follows:

(a) Let the π^0 lifetime ($\tau_{\pi^0} = 8.4 \pm .06 \times 10^{-17}$ s) represent a number $N_{\pi q}$ of quion periods, ($2\pi r_q/c' = 1.81 \times 10^{-25}$ s):

$$N_{\pi q} = \tau_{\pi^0} / (2\pi r_q / c') = 4.63 \times 10^8 \quad . \quad (2.17)$$

Then ($\ln N_{\pi^0} \approx 2\pi^2$) will be taken to indicate that there is an action integral which will describe the pion structure. Thus, after differentiating and multiplying through by ($e^2/c = m_{\pi^0} c r_{o\pi} / 2 = 2m_q c' r_q / 2$), we get:

$$\int_{(2\pi r_q)}^{N_{\pi^0}(2\pi r_q)} \left(\frac{1}{2} \right) \left(\frac{(e/2)^2}{z'} \right) dt \approx \int_0^{2\pi} \left(\frac{m_\ell}{2} \right) c' r_q d\theta \quad . \quad (2.18)$$

On the left, pearl charge is ($e/2$) and the integral represents classical potential energy action required to create a pearl travelling around a quion loop, by assembly of charge from the guidewave coherence distance $N_{\pi^0}(2\pi r_q)$. In reality, the creation may be a

faster strong force process so Eq.(2.18) would represent theoretical dissipation of a pearl. However, the classical viewpoint allows visualisation and ensures conservation of energy and action. Distance ($z' = c't$) employs velocity [$c' = c(\pi/2)$]. The right side represents kinetic energy action of a pearl as it travels at velocity c' over one quion revolution $2\pi r_q$. Only mass ($m_\ell/2$) is involved because half of the pearl mass is in the external field which does not rotate. If Eq.(2.18) were multiplied by ($\delta = h'/h$) as in Eq.(2.15) then it would represent just the associated guidewave creation mechanism.

(b) The π^+ lifetime ($\tau_{\pi^+} = 2.6033 \times 10^{-8}$ s) may also represent a number of quion periods,

$$N_{\pi^+} = (\tau_{\pi^+}) / (2\pi r_q / c') = 1.437 \times 10^{17} \quad . \quad (2.19)$$

Thus ($\ln N_{\pi^+} \approx 4\pi^2$) may be developed into an action integral similar to Eq.(2.18), but with double the action on the right, which is now expressed in terms of the quion kinetic energy action:

$$\int_{(2\pi r_q)}^{N_{\pi^+}(2\pi r_q)} \left(\frac{1}{2} \right) \left(\frac{(e/2)^2}{z'} \right) dt \approx \int_0^{2\pi} \left(\frac{m_q}{2} \right) c' r_q d\theta \quad . \quad (2.20)$$

However, the *extended* π^+ lifetime relative to π^0 should probably be attributed to the heavy-positron orbit period ($2\pi r_h / c$), in some manner like the following. Let:

$$N_p = (\tau_{\pi^+}) / (2\pi r_h / c) = 3.963 \times 10^{15} \quad ; \quad (2.21a)$$

then,

$$\ln(N_p) \approx 2\pi(137/24) \quad . \quad (2.21b)$$

Upon differentiating and multiplying through by ($e^2/c = m_{\pi^0} c r_{o\pi} / 2$), this expression could represent an action integral, such as:

$$\left(\frac{1}{137} \right) \int_{2\pi r_h}^{N_p(2\pi r_h)} \left(\frac{1}{2} \right) \left(\frac{e^2}{z} \right) dt \approx \left(\frac{1}{24} \right) \int_0^{2\pi} \left(\frac{m_{\pi^0}}{2} \right) c r_{o\pi} \frac{d\theta}{2} \quad . \quad (2.22)$$

On the left is potential energy action required to establish one of the 137 pearls (see Paper 2) within the orbiting heavy positron core, operating over guidewave coherence distance $N_p(2\pi r_h)$ at velocity c , in time τ_{π^+} . On the right side is a quantity of kinetic energy action due to one of the 24 pearl-seeds per quion over half a pion period. This expression appears to relate the establishment of the orbiting positron's internal

mechanism to the pion's existing core mechanism, through some spiralling feeler guidewave link. It is this physical linkage, plus that described in Eq.(2.15), which could then govern the long decay lifetime until guidewave coherence is broken by random peaks in the internal quantum fluctuations.

3 Various light unflavoured mesons

Design structures for a few light mesons will now be outlined, using concepts developed for models of the pion, proton and neutron. The decay products can retain some features from their parent and are simpler in design, as would be expected from a self-controlled relaxation process.

3.1 Some $J = 0$ mesons

3.1a Eta-meson: $\eta(548)$: $m = 547.853\text{MeV}/c^2$, $I^G(J^{PC}) = 0^+(0^{-+})$.

The lowest η -meson has the mass of around 4 pions, and is thought to take the basic design of a pion, see Figure 3.1a. Here the positive quion consists of 2 pearls of approximately pionic mass each; likewise for the negative anti-quion. Analogous to Eqs.(2.7)(2.8), we have:

$$m_{\eta} = 2m_q = 547.853 \pm 0.12 \text{ MeV}/c^2 , \quad (3.1.1a)$$

and approximate quion mass,

$$m_q \approx 2 \left[m_{\mu}' \left(1 - \frac{1}{37.7} \right) \right] , \quad (3.1.1b)$$

where ($m_{\mu}' = 4m_{\mu}/3$), which will be called a muonet like a miniaturised muon, as it will be used frequently later. This reveals an overall binding mass decrement due to an attractive field inside the meson. Particle core radius is given by:

$$r_{o\eta} = 2(e^2 / m_{\eta}c^2) = 5.257 \times 10^{-3} \text{ fm} , \quad (3.1.2a)$$

and quion radius is,

$$r_q = r_{o\eta} (2/\pi) . \quad (3.1.2b)$$

Apparently, there were 37 original pearl-seed particles, and the pearl radius is 37.7 times less than the real quion radius (r_q):

$$r_{\ell} = r_q / 37.7 . \quad (3.1.3)$$

Although each pearl in a quion has roughly the mass of a pion, it is miniaturised and cannot have identical design. The original 37 pearl-seeds in a quion are proposed to have condensed into 2 pearls comprising 37 gluon-loops, each of mass $m_q/(2 \times 37.7)$.

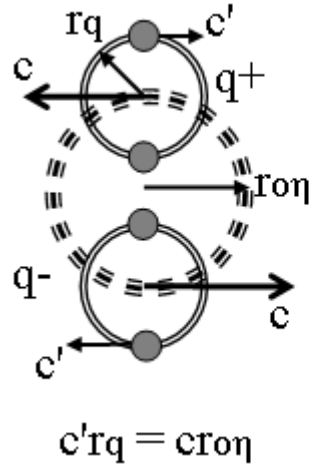


Fig.(3.1a)
Component
parts for
 $\eta(548)$

If the lifetime of an η -meson ($\tau_\eta = \hbar/\Gamma = 5.063 \times 10^{-19}$ s) is related to its core period ($2\pi r_{o\eta}/c = 11.02 \times 10^{-26}$ s), then:

$$N_\eta = \tau_\eta / (2\pi r_{o\eta}/c) = 4.59 \times 10^6, \quad (3.1.4a)$$

and,

$$\ln(N_\eta) = 15.34 = \pi^2 (\pi/2) \quad . \quad (3.1.4b)$$

After differentiation, this with Eqs.(3.1.2a), can be reduced to an integral representing the action of creation (or dissipation):

$$\int_{2\pi r_{o\eta}}^{N_\eta(2\pi r_{o\eta})} \left(\frac{1}{2}\right) \frac{e^2}{z'} dt \approx \left(\frac{\pi}{2}\right) \times \int_0^{2\pi} \left(\frac{m_q}{2}\right) c r_{o\eta} d\theta \quad . \quad (3.1.5)$$

On the left is the amount of potential energy action required to create (or dissipate) a quion travelling around the spin-loop, by assembly of charge from the guidewave coherence distance $N_\eta(2\pi r_{o\eta})$. Distance ($z' = c't$) may describe a spiral, and $(c'\tau_\eta)$ represent a guidewave coherence length. The integral on the right is a quantity of kinetic action for a quion as it travels at velocity c over one revolution ($2\pi r_{o\eta}$). Coefficient $(\pi/2)$ must be for weighting.

An η -meson may emit an attractive nuclear-type of field similar to the pion. The corresponding hard-core metric tensor component is like Eq (2.5), wherein $r_{o\pi}$ is

replaced by $r_{0\eta}$. Similarly in Eq (2.6), m_{π^0} is replaced by m_η and $a_{\chi\pi}$ by $(a_{\chi\eta} = (\chi_\eta \hbar c)^{1/2})$ for $(\chi_\eta \approx (1+0.5/137)/137)$ derived from Eq.(2.4a) after replacements. Overall empirical potential energy ($a_{\chi\eta} V_{hc}$) as a function of radius is illustrated in Figure 3.1b. It is 4 times deeper in the short range, than the pion potential of Figure 2.2. For ηN interactions, the coupling constant will be:

$$\chi_{\eta N} = (\chi_N \chi_\eta)^{1/2} \approx (9/137) \approx 0.065 \quad . \quad (3.1.6)$$

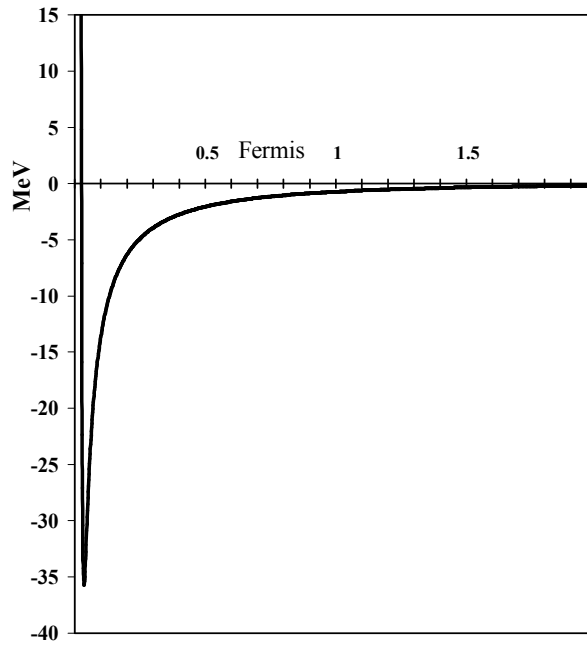


Fig.(3.1b) Hadronic potential energy function for $\eta(548)$.

3.1b $\eta'(958)$: $m = 957.78 \text{MeV}/c^2$, $I^G(J^{PC}) = 0^+(0^{-+})$

This eta-meson has a mass of around 7 pions and decays predominantly into $\eta(548)$ plus $\pi^+\pi^-$ or $\pi^0\pi^0$, which implies that it has a similar but more elaborate design than $\eta(548)$, see Figure 3.1c. In this case, the quions and anti-quion have 3 pearls each, like a trineon in a proton. However, there is a further pearl at the centre with mass that is less than the quion pearls, estimated as follows.

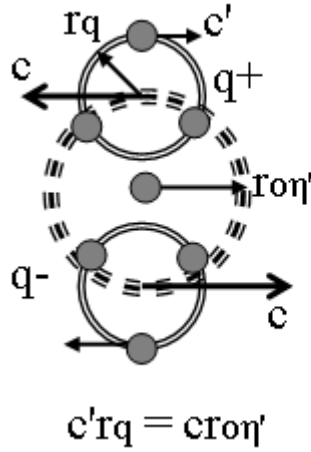


Fig.(3.1c)
Component
parts for
 $\eta'(958)$

Analogous to Eq.(3.1.1b), let the quion mass be given by:

$$m_q \approx 3 \left[m'_\mu \left(1 - \frac{1}{37.7} \right) \right] = 3 \times 137.140922 \text{ MeV} / c^2, \quad (3.1.7)$$

Factor 37.7 in the denominator means there were originally 37 pearl-seeds, and these condensed into 3 pearls, each comprising 37 gluon-loops. Pearl radius is 37.7 times less than quion radius. Now let the central pearl mass be less than a quion pearl mass, in view of its central bound position:

$$m_{cl} \approx \left[m'_\mu \left(1 - \frac{1}{24} \right) \right] = 135.007913 \text{ MeV} / c^2. \quad (3.1.8)$$

The total meson mass is therefore approximately:

$$m_{\eta'} \approx 2m_q + m_{cl} = 957.85 \text{ MeV} / c^2. \quad (3.1.9)$$

Given that the quion's pearls consist of matter, and the anti-quion's pearls of anti-matter, it appears that the central pearl must resemble a pion with its quion and anti-quion components.

Particle core radius $r_{0\eta'}$ is determined by the quion masses *without* the central pearl:

$$r_{0\eta'} = 2(e^2 / 2m_q c^2) = 3.505 \times 10^{-3} \text{ fm}, \quad (3.1.10a)$$

and the quion radius is,

$$r_q = r_{0\eta'} (2/\pi). \quad (3.1.10b)$$

Lifetime is given by ($\tau_{\eta'} = \hbar / \Gamma = 3.26 \times 10^{-21} \text{ s}$), and may be related to the quion period ($2\pi r_q / c' = 2.97 \times 10^{-26} \text{ s}$), thus:

$$N_{\eta'} = \tau_{\eta'} / (2\pi r_q / c') = 1.096 \times 10^5, \quad (3.1.11a)$$

and then,

$$\ln(N_{\eta'}) = 11.60 \approx (7/6)\pi^2. \quad (3.1.11b)$$

After differentiation, this with Eqs.(3.1.10a,b), may be reduced to an integral for action of creation (or dissipation) of the quion/anti-quion, plus a central pearl:

$$\int_{2\pi r_q}^{N_{\eta'}(2\pi r_q)} \left(\frac{1}{2}\right) \frac{e^2}{z'} dt \approx \left(\frac{7}{6}\right) \times \int_0^{2\pi} \left(\frac{m_q}{2}\right) c' r_q d\theta. \quad (3.1.12)$$

On the left is potential energy action required to create a quion, rotating at velocity c' . The guidewave coherence distance ($z' = c't$) may describe a spiral. On the right, the integral covers the kinetic action for a quion (3 pearls) rotating at velocity c' , plus the action of half the central-pearl is included through coefficient (7/6).

3.1c $a_0(980)$: $m = 980 \text{ MeV}/c^2$, $I^G(J^{PC}) = 1^-(0^{++})$.

The $a_0(980)$ meson has zero spin and mass equal to 8 pions approximately. Since the dominant decay mode is $\eta\pi$, it is proposed to have the basic form of $\eta(548)$, but now with binary pearls, see Figure 3.1d. This produces very strong binding energy within the quion which has mass given by:

$$m_q = \frac{980 \text{ MeV}/c^2}{2} \approx 4 \left[m'_\mu \left(1 - 2 \frac{(3/2)}{24} \right) \right]. \quad (3.1.13a)$$

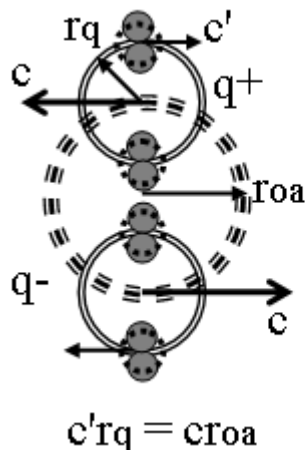


Fig.(3.1d)
Component
parts for
 $a_0(980)$

Factor (3/2)/24 signifies binding energy, and (1/24) could be a preferred pearl size relative to a quion. During creation there were probably 24 pearl-seeds, which condensed into the two pearls per quion. If the pearls rotate parallel to their quion rotation, it could increase the mass over the $f_0(980)$ with its anti-parallel rotation, say.

This would be one way of distinguishing the $a_0(980)$ from $f_0(980)$, as appears necessary according to Scadron et al. (2003), Janssen et al. (1994), Baru et al. (2003, 2008), Wang & Yang (2005).

Core radius of the $a_0(980)$ is given by:

$$r_{oa} = 2(e^2 / m_a c^2) \quad , \quad (3.1.13b)$$

and the quion radius is,

$$r_q = r_{oa} (2 / \pi) \quad . \quad (3.1.13c)$$

Lifetime ($\tau_a = \hbar / \Gamma = 8.8 \times 10^{-24}$ s) appears to be related to the core period ($2\pi r_{oa} / c = 6.13 \times 10^{-26}$ s) rather than the quion period:

$$N_a = \tau_a / (2\pi r_{oa} / c) = 143 \quad , \quad (3.1.14a)$$

and then,

$$\ln(N_a) = 4.955 \approx \pi^2 / 2 \quad . \quad (3.1.14b)$$

After differentiation, this with Eq.(3.1.13b) may be reduced to an action equation, similar in part to Eq.(3.1.5):

$$\int_{2\pi r_{oa}}^{N_a(2\pi r_{oa})} \left(\frac{1}{2} \right) \frac{e^2}{z'} dt = \int_0^{2\pi} \left(\frac{m_q}{2} \right) c r_{oa} \frac{d\theta}{2} \quad . \quad (3.1.15)$$

On the left is potential energy action required to create (or dissipate) a quion, where distance ($z' = c't$) may describe a spiral. On the right, the integral covers the kinetic action for a quion, travelling at velocity c around half the core circumference (πr_{oa}).

3.1d $f_0(980)$: $m = 980 \text{ MeV}/c^2$, $I^G(J^{PC}) = 0^+(0^{++})$.

The $f_0(980)$ meson probably has structure very similar to $a_0(980)$, but with the pearls spinning anti-parallel to their quion rotation, to reduce the overall mass below $a_0(980)$. The dominant decay ($\pi\pi$) would exclude (η) because of this anti-parallel spin.

3.2 Some mesons with ($J = 1$)

3.2a Rho-meson $\rho(770)$: $m = 775.49 \text{ MeV}/c^2$, $I^G(J^{PC}) = 1^+(1^{--})$

The $\rho(770)$ meson is distinctly different from the π and η -mesons because of its spin being $J = 1\hbar$ rather than zero. If, like other particles, only half its mass is contained in the spin-loop and half is field energy which does not rotate, then:

$$J = (m_\rho / 2)cr_\rho = \hbar \quad . \quad (3.2.1)$$

Spin-loop radius r_ρ is therefore:

$$r_\rho = 2(\hbar / m_\rho c) = 137[2(e^2 / m_\rho c^2)] \quad , \quad (3.2.2)$$

which is 137 times the classical/theoretical radius for a quion/anti-quion pair in rotation. The mass is around that of 6 pions and is thought to take the design of 3 pearls in the quion and 3 in the anti-quion, as shown in Figure 3.2a. Therefore:

$$m_q = \frac{775.49 \pm 0.34 \text{MeV} / c^2}{2} \approx 3m_{\pi_0} \left(1 - \frac{1}{24}\right) \quad , \quad (3.2.3)$$

where m_{π_0} is the "pionet" mass like a miniaturised pion, rather than the muonet mass used previously in Eq.(3.1.1b) etc. As found for the pion pearls in Eq.(2.10), these pearls are smaller than the quion by 24 times. However, like trineons in a proton, the quions are now very much smaller than the spin-loop:

$$r_q = r_\rho / 137(2/\pi) \quad . \quad (3.2.4)$$

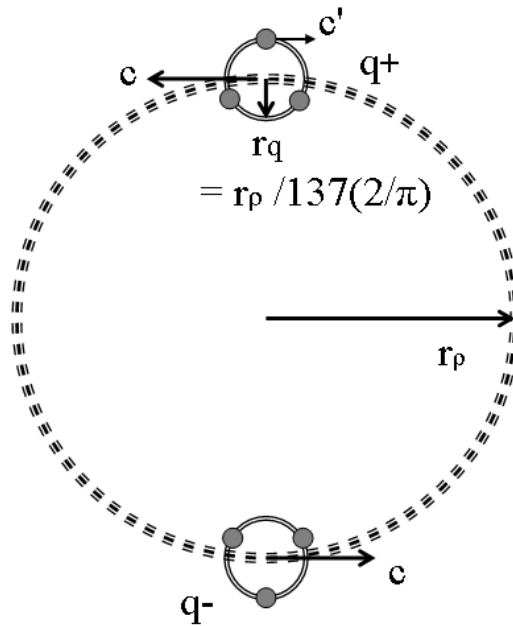


Fig.(3.2a)
Component
parts for
 $\rho(770)$

The *electromagnetic* lifetime given by ($\tau_{\rho e} = \hbar / \Gamma_{ee} = 9.35 \times 10^{-20}$ s) and the spin period ($2\pi r_\rho / c = 1.0666 \times 10^{-23}$ s) may be related by:

$$N_{\rho e} = \tau_{\rho e} / (2\pi r_\rho / c) = 8.77 \times 10^3 \quad , \quad (3.2.5a)$$

and then,

$$\ln(N_{\rho e}) = 9.079 \approx (\pi/2)(137/24) \quad . \quad (3.2.5b)$$

This may be reduced to an action integral by differentiating and introducing Eq.(3.2.2):

$$N_{\rho e(2\pi r_\rho)} \int_{2\pi r_\rho} \left(\frac{1}{2}\right) \frac{e^2}{z} dt \approx \left(\frac{1}{24}\right) \left(\frac{1}{2}\right) \int_0^{2\pi} \left(\frac{m_q}{2}\right) c r_\rho \frac{d\theta}{2} . \quad (3.2.6)$$

On the left is the potential energy action required to create (or dissipate) a quion; where $(z = ct)$ describes a spiral over a guidewave coherence length. The integral on the right side represents kinetic energy action of the quion travelling around half the spin-loop. Coefficient $(1/24)$ means that the quion originally comprised 24 pearl-seeds, but the action of only one is involved here. These 24 pearl-seeds condensed into 3 pearls, each containing 24 grains of reduced mass.

The full width $(\Gamma_\rho = 149.4 \pm 1.0 \text{ MeV})$ implies a strong lifetime $(\tau_\rho = 4.406 \times 10^{-24} \text{ s})$, which is less than the spin period given above and may be related to the period of the rotating quion $(2\pi r_q / c' = 7.783 \times 10^{-26} \text{ s})$:

$$N_{\rho q} = \tau_\rho / (2\pi r_q / c') = 56.6 , \quad (3.2.7a)$$

and then,

$$\ln(N_{\rho q}) = 4.036 = 0.41\pi^2 . \quad (3.2.7b)$$

Upon differentiating and applying Eqs.(3.2.2), (3.2.4), this reduces to an interesting action integral:

$$N_{\rho q(2\pi r_q)} \int_{2\pi r_q} \left(\frac{1}{2}\right) \frac{e^2}{z'} dt \approx \left(\frac{1}{2}\right) \int_0^{2\pi} \left(\frac{m_q}{2}\right) c' r_q \frac{d\theta}{3} . \quad (3.2.8)$$

On the left is potential energy action required to create (or dissipate) a quion; where $(z' = c't)$ over the guidewave coherence length. The integral on the right side represents kinetic energy action of a spinning quion over one third period $(2\pi r_q / 3)$.

3.2b Omega-meson: $\omega(782)$: $m = 782.65 \text{ MeV}/c^2$, $I^G(\mathbf{J}^{PC}) = 0^-(1^-)$

The $\omega(782)$ meson design is similar to $\rho(770)$, see Figure 3.2b, but with a spin-loop radius slightly less:

$$r_\omega = 2(\hbar / m_\omega c) = 137[2(e^2 / m_\omega c^2)] , \quad (3.2.9)$$

and a corresponding quion radius,

$$r_q = r_\omega / 137(2/\pi) . \quad (3.2.10)$$

The mass is again around that of 6 pionets, although the binding energy within the quions is a little less:

$$m_q = \frac{782.65 \pm 0.12 \text{ MeV} / c^2}{2} \approx 3m_{\pi_0} \left(1 - \frac{1}{37.7}\right) \left(1 - \frac{1}{137}\right). \quad (3.2.11)$$

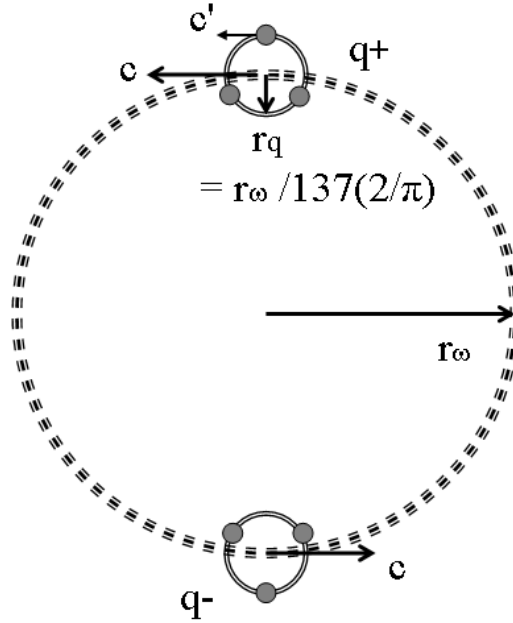


Fig.(3.2b)
Component
parts for
 $\omega(782)$

Electromagnetic lifetime ($\tau_{\omega e} = \hbar / \Gamma_{ee} = 1.10 \times 10^{-18} \text{ s}$) appears to be related to the spin period ($2\pi r_\omega / c = 1.056 \times 10^{-23} \text{ s}$) by:

$$N_{\omega e} = \tau_{\omega e} / (2\pi r_\omega / c) = 1.041 \times 10^5 ; \quad (3.2.12a)$$

and then,

$$\ln(N_{\omega e}) = 11.55 \approx \pi(137/37.7) . \quad (3.2.12b)$$

By differentiating and introducing Eq.(3.2.9), this may be reduced to an action integral:

$$N_{\omega e} \int_{2\pi r_\omega}^{2\pi r_\omega} \left(\frac{1}{2}\right) \frac{e^2}{z} dt \approx \left(\frac{1}{37.7}\right) \int_0^{2\pi} \left(\frac{m_q}{2}\right) c r_\omega \frac{d\theta}{2} . \quad (3.2.13)$$

On the left is potential energy action required to create (or dissipate) a quion; where ($z = ct$) could describe a spiral over the guidewave coherence length. The integral on the right side represents kinetic energy action of the quion as it travels around half the spin-loop. Factor 37.7 in the denominator means there were originally 37 pearl-seeds and only one is being considered. These 37 pearl-seeds condensed into 3 pearls, each containing 37 grains of reduced mass.

Full width ($\Gamma_\omega = 8.49 \pm 0.08$ MeV) implies a strong lifetime ($\tau_\omega = 7.75 \times 10^{-23}$ s), which may be related to one third of a quion's rotation period ($2\pi r_q/3c' = 2.57 \times 10^{-26}$ s):

$$N_{\omega q/3} = \tau_\omega / (2\pi r_q / 3c') = 3016 \quad . \quad (3.2.14a)$$

Then,

$$\ln(N_{\omega q/3}) = 8.01 = 0.81\pi^2 \quad , \quad (3.2.14b)$$

and upon differentiating and introducing Eqs.(3.2.9) and (3.2.10), this reduces to an interesting action integral:

$$\int_{(2\pi r_q/3)}^{N_{\omega q/3}(2\pi r_q/3)} \left(\frac{1}{2}\right) \frac{e^2}{z'} dt \approx \int_0^{2\pi} \left(\frac{m_q}{2}\right) c' r_q \frac{d\theta}{3} \quad . \quad (3.2.15)$$

On the left is potential energy action required to create (or dissipate) a quion; where ($z' = c't$) over the guidewave coherence length. The integral on the right side represents kinetic energy action of a spinning quion over one third of a revolution ($2\pi r_q/3$). Equation (3.2.14a) implies that a third harmonic guidewave is operating around the quion.

3.2c Phi-meson $\phi(1020)$: $m = 1019.455 \text{MeV}/c^2$, $I^G(J^{PC}) = 0^-(1^-)$.

The $\phi(1020)$ meson has spin $1\hbar$ given by:

$$J = (m_\phi / 2) c r_\phi = \hbar \quad , \quad (3.2.16)$$

where spin-loop radius r_ϕ is:

$$r_\phi = 137[2(e^2 / m_\phi c^2)] \quad , \quad (3.2.17)$$

and quion radius,

$$r_q = r_\phi / 137(2/\pi) \quad . \quad (3.2.18)$$

Mass is approximately that of 8 pionets and is to take the form of 4 pearls in the quion and 4 in the antiquion, as shown in Figure 3.2c. During decay these usually convert to separate kaons, although a rho + pi is also possible. Quion mass is given by:

$$m_q = \frac{1019.455 \text{MeV}/c^2}{2} \approx 4m_{\pi_0} \left(1 - \frac{(4/3)(3/2)}{37.7}\right) \quad . \quad (3.2.19)$$

The constituent pearls are smaller than the quion by 37.7 times. Factor (4/3) means that three pearls are at the vertices of an equilateral triangle, and the fourth at the centre, see Simo (1978). Again, the quions are $137(2/\pi)$ times smaller than the spin-

loop, like trineons in a proton. This ensures that a quion rotates 137 times at velocity c' during one spin-loop orbit, which is a stable arrangement.

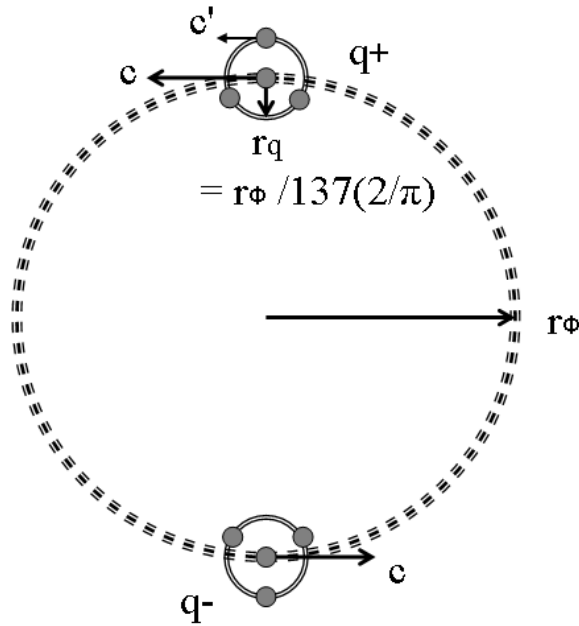


Fig.(3.2c)
Component
parts for
 $\Phi(1020)$

The electromagnetic lifetime given by ($\tau_{\phi e} = \hbar / \Gamma_{ee} = 5.183 \times 10^{-19}$ s) and the spin period ($2\pi r_{\phi} / c = 8.114 \times 10^{-24}$ s) may be related by:

$$N_{\phi} = \tau_{\phi e} / (2\pi r_{\phi} / c) = 6.388 \times 10^4 \quad , \quad (3.2.20a)$$

and,

$$\ln(N_{\phi e}) = 11.065 \approx \pi(137/37.7) \quad . \quad (3.2.20b)$$

This can be differentiated and, with Eq.(3.2.17), reduced to an action integral similar to Eq.(3.2.13):

$$\int_{2\pi r_{\phi}}^{N_{\phi e}(2\pi r_{\phi})} \left(\frac{1}{2} \right) \frac{e^2}{z} dt \approx \left(\frac{1}{37.7} \right) \int_0^{2\pi} \left(\frac{m_q}{2} \right) c r_{\phi} \frac{d\theta}{2} \quad . \quad (3.2.21)$$

On the left is potential energy action required to create a quion, where ($z = ct$) along a spiral over the guidewave coherence length. The integral on the right represents kinetic energy action of the quion as it travels around half the spin-loop. Denominator 37.7 means that only one of the 37 pearl-seeds is being considered. These 37 pearl-seeds condensed into 3 pearls, each containing 37 less-massive grains.

The full width ($\Gamma_{\phi} = 4.26 \pm 0.04$ MeV) implies a strong lifetime of ($\tau_{\phi} = 1.55 \times 10^{-22}$ s). This lifetime may be related to the period of the rotating quion ($2\pi r_q / c' = 5.921 \times 10^{-26}$ s):

$$N_\phi = \tau_\phi / (2\pi r_q / c') = 2618 \quad , \quad (3.2.22a)$$

and then,

$$\ln(N_\phi) = 7.87 = 0.80\pi^2 \quad . \quad (3.2.22b)$$

Upon differentiating and introducing Eqs.(3.2.17) and (3.2.18), this reduces to an action integral:

$$\int_{2\pi r_q}^{N_\phi(2\pi r_q)} \left(\frac{1}{2}\right) \frac{e^2}{z'} dt \approx \int_0^{2\pi} \left(\frac{m_q}{2}\right) c' r_q \frac{d\theta}{3} \quad . \quad (3.2.23)$$

On the left is potential energy action expended to create (or dissipate) a quion; where $z' = c't$ over the guidewave coherence length. The integral on the right side represents kinetic energy action of a spinning quion over one third revolution ($2\pi r_q / 3$).

4 General design of light unflavoured mesons

In the previous section, the very lightest mesons have been described in some detail, but more massive mesons of each species have also been studied in order to produce similar viable structures. Choice of design has been based upon the belief that the decay process is a relaxation effect so that the products should be simpler, but retain some of the parent features. Those decays accompanied by low levels of kinetic energy are most likely to satisfy this criterion. Pearls are not created during a decay process, so the number of pearls will either stay the same or decrease by annihilation. It is easy for the pearl type to remain unchanged or to lose energy by changing from muonet ($m_\mu' = 140.9\text{MeV}/c^2$) to pionet ($m_{\pi_0} = 135\text{MeV}/c^2$); but less easy for the reverse process, except when enough free kinetic energy is accessible. These rules restrict the use of m_μ' to mesons with ($C = +1, (\pi \eta \text{ a f})$), and m_{π_0} to mesons with ($C = -1, (\rho \omega \phi \text{ b h})$).

The mesons occupy 8 categories and have been listed with regard to their properties in Table 4.1. They have 5 defining characteristics, $I^G J^P C$. Each class has a particular parity P with a free choice of J value, but I, G and C are related through:

$$CG = 1 - 2I \quad , \quad (4.1)$$

which limits the number of classes to 8 only. The meson traditional nomenclature is: (a) Pseudoscalar ($J^P = 0^-$). (b) Scalar ($J^P = 0^+$). (c) Pseudovector ($J^P = 1^+$). (d) Vector ($J^P = 1^-$).

Table 4.1 Classification of the light unflavoured mesons.

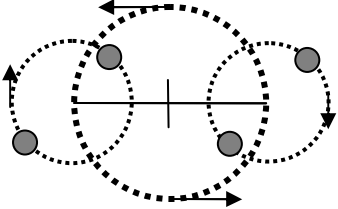
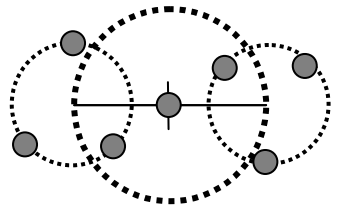
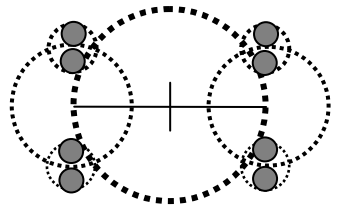
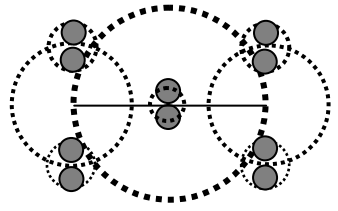
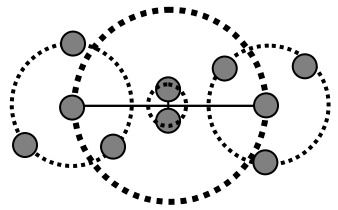
J^{PC}	J^{-+}			J^{++}				J^{--}		J^{+-}
	0^{-+}	1^{-+}	2^{-+}	0^{++}	1^{++}	2^{++}	4^{++}	1^{--}	3^{--}	1^{+-}
<u>I=1</u>	<u>G=-1</u>			<u>G=-1</u>				<u>G=+1</u>		<u>G=+1</u>
	π^0			$a_0(980)$				$\rho(770)$		$b_1(1235)$
	$\pi(1300)$			$a_1(1260)$				$\rho(1450)$		
	$\pi_1(1400)$			$a_2(1320)$				$\rho_3(1690)$		
	$\pi_1(1600)$			$a_0(1450)$				$\rho(1700)$		
	$\pi_2(1670)$					$a_4(2040)$				
	$\pi(1800)$									
	$\pi_2(1880)$									
<u>I=0</u>	<u>G=+1</u>			<u>G=+1</u>				<u>G=-1</u>		<u>G=-1</u>
	$\eta(548)$			$f_0(980)$				$\omega(782)$		$h_1(1170)$
	$\eta'(958)$				$f_2(1270)$			$\phi(1020)$		
	$\eta(1295)$			$f_1(1285)$				$\omega(1420)$		
	$\eta(1405)$			$f_0(1370)$				$\omega(1650)$		
	$\eta(1475)$			$f_1(1420)$				$\omega_3(1670)$		
	$\eta_2(1645)$			$f_0(1500)$				$\phi(1680)$		
					$f_2'(1525)$			$\phi_3(1850)$		
				$f_0(1710)$						
					$f_2(1950)$					
					$f_2(2010)$					
					$f_4(2050)$					
					$f_2(2300)$					
					$f_2(2340)$					

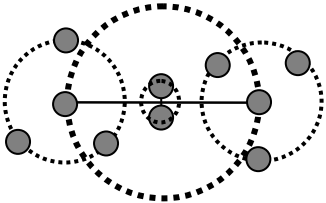
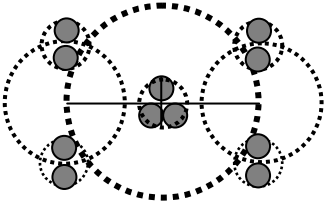
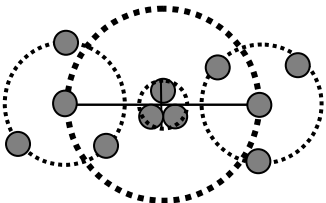
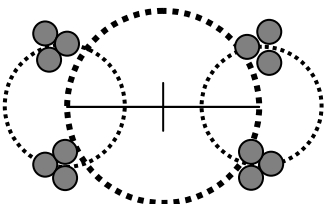
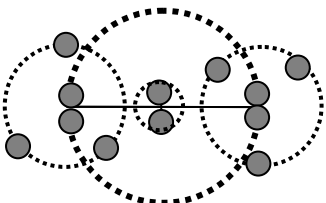
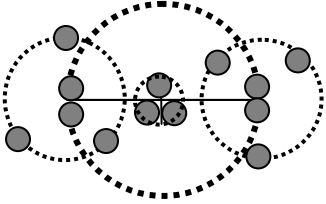
Scalar and pseudoscalar mesons with zero angular momentum appear to be tight orbiting structures, consisting of discrete pearls of muonnet-mass around $140.9\text{MeV}/c^2$, see Table 4.2. The quion and anti-quion rotate counter to their orbital motion, in order to cancel angular momentum overall, as in Eq.(2.1) and Section 3.1. All vector and pseudo-vector mesons ($J \geq 1$) appear to be open structures, to generate the spin, following Eq.(3.2.1). Some of these mesons also consist of m_μ' - pearls, as listed in Table 4.3. The others consist of pearls of pionet-mass ($134.9776\text{MeV}/c^2$), and decay into simpler pionic structures; see Table 4.4.

Mesons $f_1(1285)$, $\eta(1295)$, $\eta(1405)$, $\eta(1475)$, and $\pi(1800)$ can decay into $a_0(980)$, so they have the same unusual twin-pearl structure, based on the inheritance principle.

The mass decrements indicate the degree of binding overall and in some cases the size of the pearls relative to their quion size, as in Section 2.2.

Table 4.2 Internal designs for scalar and pseudoscalar mesons, comprising pearls of muonet-mass ($m_{\mu'} = 140.877823\text{MeV}/c^2$), approximately. A mass analysis formula is given, plus $I^G(J^{PC})$, full width Γ , and the main decay products $Dy(\dots)$.

<p>$4\mu'$</p> 	<p>$\eta(548) / 547.853 \pm 0.024 \text{ MeV}$ $0^+(0^-+), \Gamma = 1.29\text{keV}, Dy(3\pi, 2\gamma)$</p> $m \approx 4m'_{\mu} \left(1 - \frac{1}{37.7} \right)$ $= 548.56\text{MeV}$
<p>$7\mu'$</p> 	<p>$\eta'(958) / 957.78 \pm 0.06 \text{ MeV}$ $0^+(0^-+), \Gamma = 0.202 \text{ MeV}, Dy(\pi, \eta, \rho, \omega)$</p> $m \approx 6m'_{\mu} \left(1 - \frac{1}{37.7} \right) + m'_{\mu} \left(1 - \frac{1}{24} \right)$ $= 957.85\text{MeV}$
<p>$8\mu'$</p> 	<p>$a_0(980) / 980 \pm 20 \text{ MeV}$ $1^-(0^++), \Gamma = 50\text{-}100 \text{ MeV}, Dy(\eta\pi)$</p> <p>$f_0(980) / 980 \pm 10 \text{ MeV}$ $0^+(0^++), \Gamma = 40\text{-}100 \text{ MeV}, Dy(\pi\pi)$</p> $m \approx 8m'_{\mu} \left(1 - \frac{2(3/2)}{24} \right) = 986.1\text{MeV}$
<p>$10\mu'$</p> 	<p>$\eta(1295) / 1294 \pm 4 \text{ MeV}$ $0^+(0^-+), \Gamma = 55 \text{ MeV}, Dy(a_0(980), \eta)$</p> $m \approx 8m'_{\mu} \left(1 - \frac{2}{24} \right) + 2m'_{\mu} \left(1 - \frac{(3/2)}{24} \right)$ $= 1297.2\text{MeV}$
<p>$10\mu'$</p> 	<p>$\pi(1300) / 1300 \pm 100 \text{ MeV}$ $1^-(0^-+), \Gamma = 200\text{-}600 \text{ MeV}, Dy(\rho\pi)$</p> $m \approx 8m'_{\mu} \left(1 - \frac{(4/3)(3/2)}{24} \right) + 2m'_{\mu} \left(1 - \frac{1}{24} \right)$ $= 1303.1\text{MeV}$

<p>10μ'</p> 	<p>$f_0(1370)$ / 1350 ± 150 MeV $0^+(0^{++})$, $\Gamma = 200\text{-}500$ MeV, Dy($\pi\pi, \eta\eta, K\tilde{K}$). $m \approx 8m'_\mu \left(1 - \frac{(4/3)}{37.7}\right) + 2m'_\mu \left(1 - \frac{(3/2)}{24}\right)$ $= 1351.3\text{MeV}$</p>
<p>11μ'</p> 	<p>$\eta(1405)$ / 1409.8 ± 2.5 MeV $0^+(0^{-+})$, $\Gamma = 51$ MeV, Dy($\eta, K\tilde{K}, a_0(980)$). $m \approx 8m'_\mu \left(1 - \frac{2}{24}\right) + 3m'_\mu \left(1 - \frac{2(3/2)}{24}\right)$ $= 1402.9\text{MeV}$</p>
<p>11μ'</p> 	<p>$a_0(1450)$ / 1474 ± 19 MeV $1^-(0^{++})$, $\Gamma = 265\text{MeV}$, Dy($\eta'(958), K\tilde{K}$) $m \approx 8m'_\mu \left(1 - \frac{(4/3)}{37.7}\right) + 3m'_\mu \left(1 - \frac{2}{24}\right)$ $= 1474.6\text{MeV}$</p>
<p>12μ'</p> 	<p>$\eta(1475)$ / 1476 ± 4 MeV $0^+(0^{-+})$, $\Gamma = 87$ MeV, Dy($K\tilde{K}\pi, a_0(980)$) $m \approx 12m'_\mu \left(1 - \frac{2(3/2)}{24}\right)$ $= 1479.2\text{MeV}$</p>
<p>12μ'</p> 	<p>$f_0(1500)$ / 1505 ± 6 MeV $0^+(0^{++})$, $\Gamma = 109$ MeV, Dy($\pi\pi, K\tilde{K}, \eta\eta, \eta\eta'(958)$) $m \approx 10m'_\mu \left(1 - \frac{(5/3)(3/2)}{24}\right) +$ $+ 2m'_\mu \left(1 - \frac{2(3/2)}{24}\right) = 1508.6\text{MeV}$</p>
<p>13μ'</p> 	<p>$f_0(1710)$ / 1720 ± 6 MeV $0^+(0^{++})$, $\Gamma = 140$ MeV, Dy($K\tilde{K}, \eta\eta, \omega\omega$) $m \approx 10m'_\mu \left(1 - \frac{5/3}{24}\right) + 3m'_\mu \left(1 - \frac{1}{24}\right)$ $= 1716.0\text{MeV}$</p>

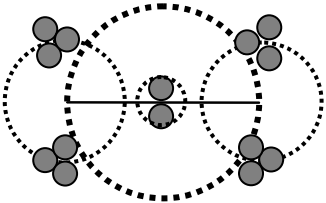
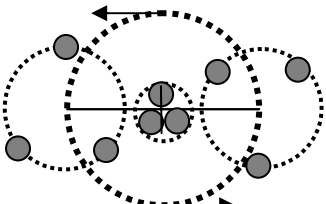
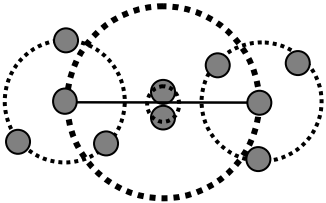
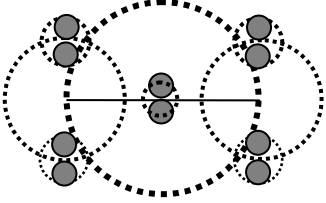
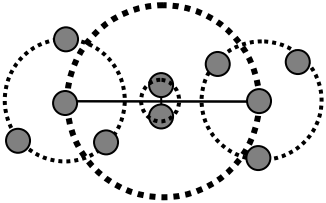
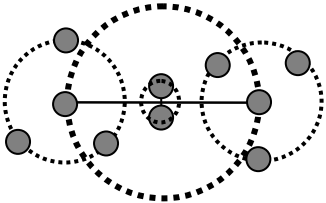
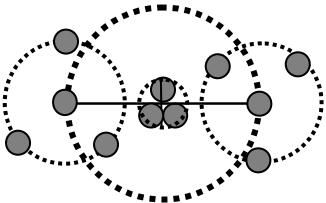
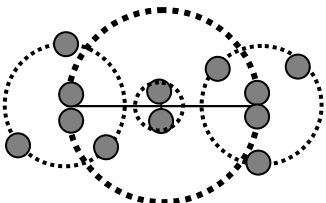
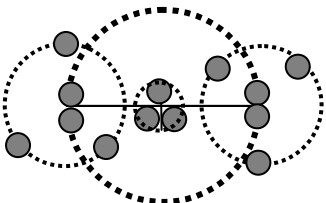
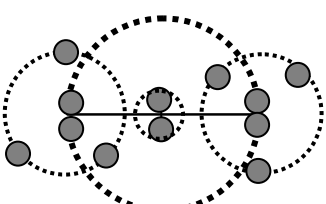
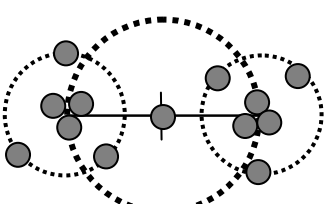
<p>14μ'</p> 	<p>$\pi(1800) / 1816 \pm 14 \text{ MeV}$ $1^-(0^-), \Gamma = 207 \text{ MeV}, \text{Dy}(a_0(980), \eta\eta'(958))$</p> $m \approx 12m'_\mu \left(1 - \frac{2}{24}\right) + 2m'_\mu \left(1 - \frac{1}{24}\right)$ $= 1819.7 \text{ MeV}$
--	---

Table 4.3 Internal designs for vector and pseudovector mesons, comprising pearls of muonet-mass m'_μ approximately.

<p>9μ'</p> 	<p>$a_1(1260) / 1230 \pm 40 \text{ MeV}$ $1^-(1^+), \Gamma = 250\text{-}600 \text{ MeV}, \text{Dy}(\rho\pi).$</p> $m \approx 6m'_\mu \left(1 - \frac{1}{37.7}\right) + 3m'_\mu \left(1 - \frac{1}{37.7}\right)$ $= 1234.3 \text{ MeV}$
<p>10μ'</p> 	<p>$f_2(1270) / 1275.1 \pm 1.2 \text{ MeV}$ $0^+(2^{++}), \Gamma = 185 \text{ MeV}, \text{Dy}(\pi\pi, K\bar{K})$</p> $m \approx 8m'_\mu \left(1 - \frac{(4/3)(3/2)}{24}\right) +$ $2m'_\mu \left(1 - \frac{2(3/2)}{24}\right) = 1279.6 \text{ MeV}$
<p>10μ'</p> 	<p>$f_1(1285) / 1281.8 \pm 0.6 \text{ MeV}$ $0^+(1^{++}), \Gamma = 24.3 \text{ MeV}, \text{Dy}(a_0(980), K\bar{K})$</p> $m \approx 8m'_\mu \left(1 - \frac{2}{24}\right) + 2m'_\mu \left(1 - \frac{2(3/2)}{24}\right)$ $= 1279.6 \text{ MeV}$
<p>10μ'</p> 	<p>$a_2(1320) / 1318.3 \pm 0.6 \text{ MeV}$ $1^-(2^{++}), \Gamma = 107 \text{ MeV}, \text{Dy}(\eta\pi, \omega\pi\pi, K\bar{K}).$</p> $m \approx 8m'_\mu \left(1 - \frac{(4/3)}{24}\right) + 2m'_\mu \left(1 - \frac{2}{24}\right)$ $= 1322.7 \text{ MeV}$

<p>10μ'</p> 	<p>$\pi_1(1400) / 1354 \pm 25 \text{ MeV}$ $1^-(1^-+), \Gamma = 313 \text{ MeV}, \text{Dy}(\eta\pi).$ $m \approx 8m'_\mu \left(1 - \frac{(4/3)}{37.7}\right) + 2m'_\mu \left(1 - \frac{1}{24}\right)$ $= 1357.2 \text{ MeV}$</p>
<p>11μ'</p> 	<p>$f_1(1420) / 1426.4 \pm 0.9 \text{ MeV}$ $0^+(1^{++}), \Gamma = 54.9 \text{ MeV},$ $\text{Dy}(\text{K}\tilde{\text{K}}^*(892), \phi)$ $m \approx 8m'_\mu \left(1 - \frac{(4/3)(3/2)}{24}\right) +$ $3m'_\mu \left(1 - \frac{(3/2)}{24}\right) = 1429.3 \text{ MeV}$</p>
<p>12μ'</p> 	<p>$f_2'(1525) / 1525 \pm 5 \text{ MeV}$ $0^+(2^{++}), \Gamma = 73 \text{ MeV}, \text{Dy}(\text{K}\tilde{\text{K}}^*, \eta\eta)$ $m \approx 10m'_\mu \left(1 - \frac{(5/3)(3/2)}{24}\right) +$ $2m'_\mu \left(1 - \frac{(3/2)}{24}\right) = 1526.2 \text{ MeV}$</p>
<p>13μ'</p> 	<p>$\pi_1(1600) / 1662 \pm 15 \text{ MeV}$ $1^-(1^-+), \Gamma = 234 \text{ MeV}, \text{Dy}(\eta'(958))$ $m \approx 10m'_\mu \left(1 - \frac{(5/3)(3/2)}{24}\right) +$ $+ 3m'_\mu \left(1 - \frac{(3/2)}{24}\right) = 1658.2 \text{ MeV}$</p>
<p>12μ'</p> 	<p>$\eta_2(1645) / 1617 \pm 5 \text{ MeV}$ $0^+(2^-+), \Gamma = 181 \text{ MeV}, \text{Dy}(a_2(1320), \text{K}\tilde{\text{K}}^*, \eta\pi)$ $m \approx 10m'_\mu \left(1 - \frac{(5/3)}{37.7}\right) + 2m'_\mu \left(1 - \frac{1}{37.7}\right)$ $= 1620.8 \text{ MeV}$</p>
<p>13μ'</p> 	<p>$\pi_2(1670) / 1672.4 \pm 3.2 \text{ MeV}$ $1^-(2^-+), \Gamma = 259 \text{ MeV}, \text{Dy}(f_2(1270), \rho, \text{K}\tilde{\text{K}}^*)$ $m \approx 12m'_\mu \left(1 - \frac{(6/3)}{24}\right) + m'_\mu \left(1 - \frac{2}{24}\right)$ $= 1678.8 \text{ MeV}$</p>

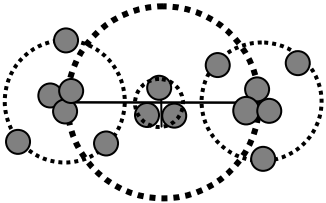
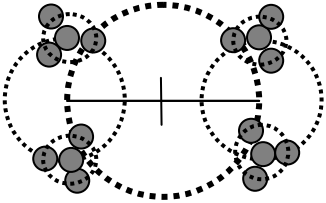
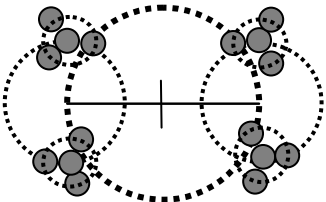
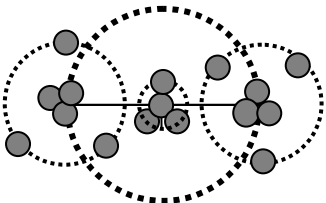
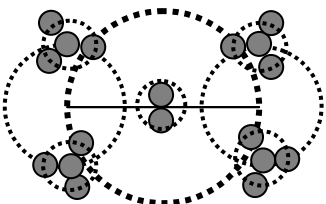
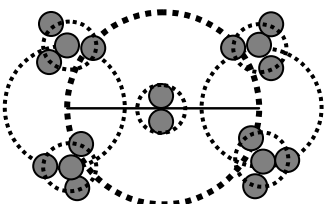
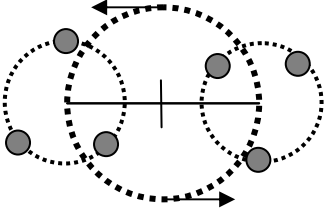
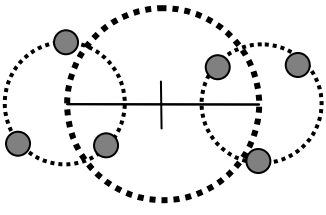
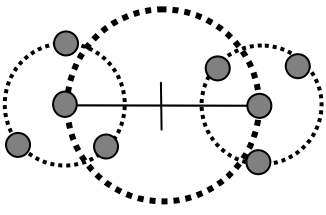
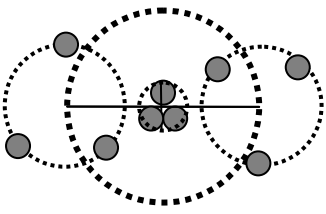
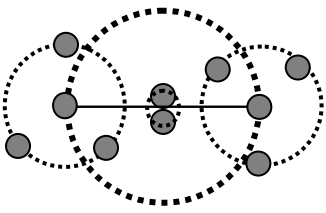
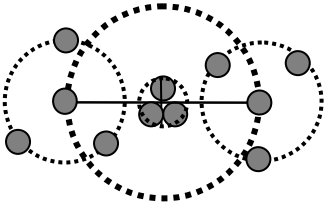
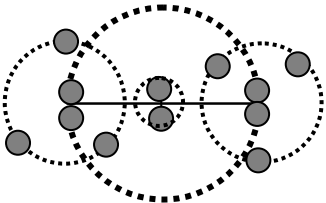
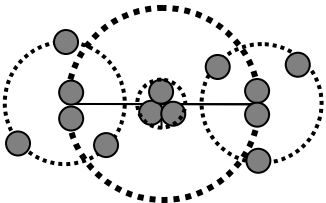
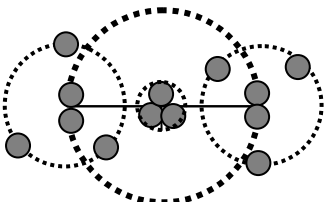
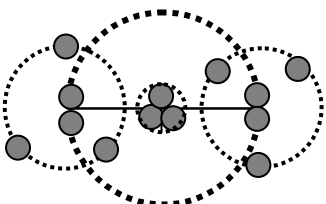
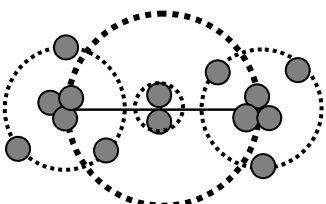
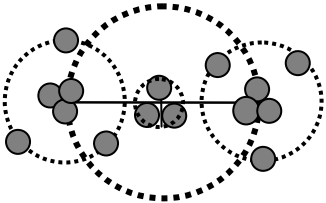
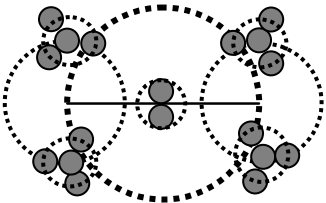
<p>15μ'</p> 	<p>$f_2(1950)$ / 1944 ± 12 MeV $0^+(2^{++})$, $\Gamma = 472$ MeV, Dy($K^* \bar{K}^*(892), \eta\eta$)</p> $m \approx 12m'_\mu \left(1 - \frac{(6/3)}{24}\right) + 3m'_\mu \left(1 - \frac{(3/2)}{24}\right)$ <p>= 1945.9 MeV</p>
<p>16μ'</p> 	<p>$f_2(2010)$ / 2011 ± 60 MeV $0^+(2^{++})$, $\Gamma = 202$ MeV, Dy($\varphi\varphi, K\bar{K}$)</p> $m \approx 16m'_\mu \left(1 - \frac{2(4/3)}{24}\right)$ <p>= 2003.6 MeV</p>
<p>16μ'</p> 	<p>$a_4(2040)$ / 2001 ± 10 MeV $1^-(4^{++})$, $\Gamma = 313$ MeV, Dy($K\bar{K}, \rho\omega, f_2(1270)$)</p> $m \approx 16m'_\mu \left(1 - \frac{2(4/3)}{24}\right)$ <p>= 2003.6 MeV</p>
<p>16μ'</p> 	<p>$f_4(2050)$ / 2018 ± 11 MeV $0^+(4^{++})$, $\Gamma = 237$ MeV, Dy($\pi\pi, K\bar{K}, \eta\eta$)</p> $m \approx 12m'_\mu \left(1 - \frac{(6/3)(3/2)}{24}\right) +$ $4m'_\mu \left(1 - \frac{(4/3)}{37.7}\right) = 2022.8 \text{ MeV}$
<p>18μ'</p> 	<p>$f_2(2300)$ / 2297 ± 28 MeV $0^+(2^{++})$, $\Gamma = 149$ MeV, Dy($\varphi\varphi, K\bar{K}$)</p> $m \approx 16m'_\mu \left(1 - \frac{2(4/3)}{24}\right) + 2m'_\mu \left(1 - \frac{1}{37.7}\right)$ <p>= 2278.0 MeV</p>
<p>18μ'</p> 	<p>$f_2(2340)$ / 2339 ± 60 MeV $0^+(2^{++})$, $\Gamma = 319$ MeV, Dy($\varphi\varphi, \eta\eta$)</p> $m \approx 16m'_\mu \left(1 - \frac{2(4/3)}{37.7}\right) +$ $+ 2m'_\mu \left(1 - \frac{2(3/2)}{24}\right) = 2341.1 \text{ MeV}$

Table 4.4 Internal designs for vector and pseudovector mesons, comprising pearls of pionet-mass ($m_{\pi_0} = 134.9776\text{MeV}$), approximately.

<p>6π</p> 	<p>$\rho(770) / 775.49 \pm 0.34 \text{ MeV}$ $1^+(1^{--}), \Gamma = 149.4 \text{ MeV}, \text{Dy}(\pi\pi).$</p> $m \approx 6m_{\pi_0} \left(1 - \frac{1}{24}\right)$ $= 776.1\text{MeV}$
<p>6π</p> 	<p>$\omega(782) / 782.65 \pm 0.12 \text{ MeV}$ $0^-(1^{--}), \Gamma = 8.49 \text{ MeV}, \text{Dy}(\pi\pi\pi).$</p> $m \approx 6m_{\pi_0} \left(1 - \frac{1}{37.7}\right)$ $= 788.4\text{MeV}$
<p>8π</p> 	<p>$\phi(1020) / 1019.455 \pm 0.020 \text{ MeV}$ $0^-(1^{--}), \Gamma = 4.26 \text{ MeV}, \text{Dy}(\text{KK}, \rho\pi).$</p> $m \approx 8m_{\pi_0} \left(1 - \frac{(4/3)(3/2)}{37.7}\right)$ $= 1022.5\text{MeV}$
<p>9π</p> 	<p>$h_1(1170) / 1170 \pm 20 \text{ MeV}$ $0^-(1^{+-}), \Gamma = 360 \text{ MeV}, \text{Dy}(\rho\pi).$</p> $m \approx 6m_{\pi_0} \left(1 - \frac{1}{24}\right) + 3m_{\pi_0} \left(1 - \frac{1}{37.7}\right)$ $= 1170.3\text{MeV}$
<p>10π</p> 	<p>$b_1(1235) / 1229.5 \pm 3.2 \text{ MeV}$ $1^+(1^{+-}), \Gamma = 142 \text{ MeV}, \text{Dy}(\omega, \text{K}\tilde{\text{K}}, \phi).$</p> $m \approx 8m_{\pi_0} \left(1 - \frac{(4/3)(3/2)}{24}\right) +$ $+ 2m_{\pi_0} \left(1 - \frac{2}{24}\right) = 1237.3\text{MeV}$

<p>11π</p> 	<p>$\omega(1420)$ / (1400-1450) MeV $0^-(1^{--})$, $\Gamma = 180\text{-}250$ MeV, Dy($b_1(1235), \rho$)</p> $m \approx 8m_{\pi_0} \left(1 - \frac{(4/3)}{37.7}\right) + 3m_{\pi_0} \left(1 - \frac{1}{24}\right)$ $= 1429.7\text{MeV}$
<p>12π</p> 	<p>$\rho(1450)$ / 1465 ± 25 MeV $1^+(1^{--})$, $\Gamma = 400$ MeV, Dy($\pi\pi$)</p> $m \approx 10m_{\pi_0} \left(1 - \frac{(5/3)(3/2)}{24}\right) +$ $2m_{\pi_0} \left(1 - \frac{1}{24}\right) = 1467.9\text{MeV}$
<p>13π</p> 	<p>$\omega(1650)$ / 1670 ± 30 MeV $0^-(1^{--})$, $\Gamma = 315$ MeV, Dy($\rho\pi, \omega\pi\pi, \omega\eta$)</p> <p>$\omega_3(1670)$ / 1667 ± 4 MeV $0^-(3^{--})$, $\Gamma = 168$ MeV, Dy(ρ, ω)</p> $m \approx 10m_{\pi_0} \left(1 - \frac{(5/3)}{37.7}\right) + 3m_{\pi_0} \left(1 - \frac{1}{24}\right)$ $= 1678.2\text{MeV}$
<p>13π</p> 	<p>$\phi(1680)$ / 1680 ± 20 MeV $0^-(1^{--})$, $\Gamma = 150$ MeV, Dy($K\tilde{K}^*(892)$)</p> $m \approx 10m_{\pi_0} \left(1 - \frac{(5/3)}{37.7}\right) + 3m_{\pi_0} \left(1 - \frac{1}{37.7}\right)$ $= 1684.3\text{MeV}$
<p>13π</p> 	<p>$\rho_3(1690)$ / 1688.8 ± 2.1 MeV $1^+(3^{--})$, $\Gamma = 161$ MeV, Dy($\pi, K\tilde{K}, \rho$)</p> $m \approx 10m_{\pi_0} \left(1 - \frac{(5/3)}{37.7}\right) + 3m_{\pi_0} \left(1 - \frac{1}{37.7}\right)$ $= 1684.3\text{MeV}$
<p>14μ'</p> 	<p>$\rho(1700)$ / 1720 ± 20 MeV $1^+(1^{--})$, $\Gamma = 250$ MeV, Dy($\rho\pi\pi, \rho\rho, K\tilde{K}$)</p> $m \approx 12m_{\pi_0} \left(1 - \frac{(6/3)}{24}\right) + 2m_{\pi_0} \left(1 - \frac{2(3/2)}{24}\right)$ $= 1721.0\text{MeV}$

<p>15μ'</p> 	<p>$\phi_3(1850) / 1854 \pm 7 \text{ MeV}$ $0^-(3^{--}), \Gamma = 87 \text{ MeV}, \text{Dy}(\text{K}\tilde{\text{K}}^*(892))$ $m \approx 12m_{\pi_0} \left(1 - \frac{(6/3)}{24}\right) + 3m_{\pi_0} \left(1 - \frac{2}{24}\right)$ $= 1855.9 \text{ MeV}$</p>
<p>18π</p> 	<p>$\phi(2170) / 2175 \pm 15 \text{ MeV}$ $0^-(1^{--}), \Gamma = 61 \text{ MeV}, \text{Dy}(\text{K}\text{K}, \phi f_0(980))$ $m \approx 16m_{\pi_0} \left(1 - \frac{2(4/3)}{24}\right) + 2m_{\pi_0} \left(1 - \frac{1}{24}\right)$ $= 2178.4 \text{ MeV}$</p>

Given all these meson designs, it is now possible to see how spin depends on mass to some extent but not predictably. Measured spin is accurately known and the number of pearls in each meson is known, but the binding energy varies greatly and causes uncertainty. Figure 4.1 shows J vs M for these meson structures, overlaid by lines of an average binding energy according to the expression:

$$M = \frac{2.75}{3} m_{\mu}' (3J + n + 3) \quad (4.2)$$

Usually, the spin J falls below the main line ($n = 0$) and can increase with mass, but it shows no obvious relationship.

In order to eliminate the confusion caused by variable binding energy, Figure 4.2 shows (J vs M) for theoretical meson structures with *negligible* binding energy, according to the expression:

$$M = m_{\mu}' (3J + n + 3) \quad (4.3)$$

There now appears to be some order which may eventually be explicable. At the low mass end, several vacancies still remain even after adding 4 strange mesons to fill gaps. The $\rho(770)$ stands out as unusual.

Missing meson resonances at ($J = 0, n = 0, 2, 3, 6$) correspond through Eq.(4.1) to reduced masses 387MeV, 646MeV($f_0(600)$), 775MeV($\kappa(800)$), 1162MeV. These controversial states are currently supported by several investigators, for example, Parganlija et al (2009).

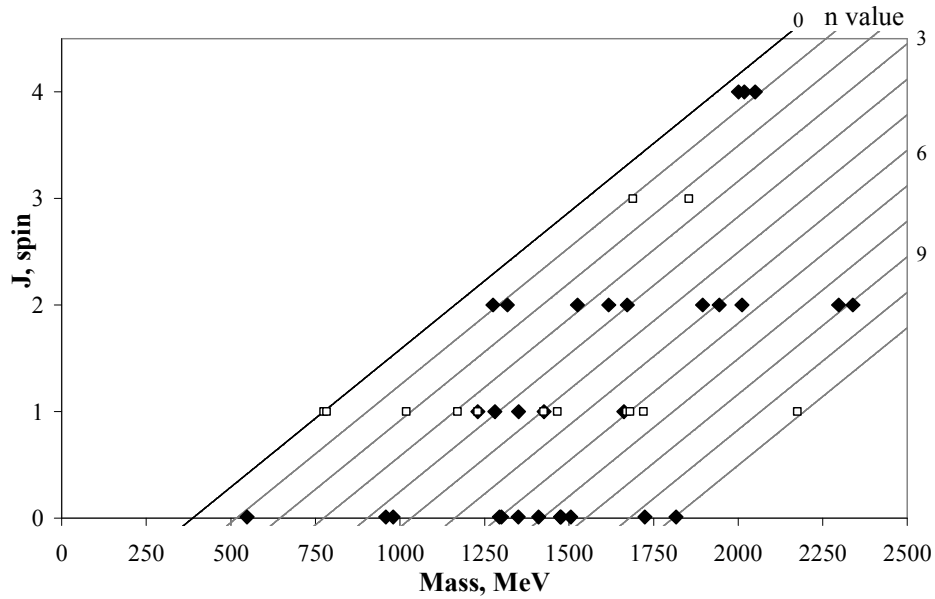


Fig.4.1 The actual relationship between spin and mass for light unflavoured mesons, with average binding energy lines overlaid according to Eq.(4.2). Factor n is given on the right ordinate. The solid points are for mesons in Tables 4.2, 4.3, and hollow points are for the mesons in Table 4.4.

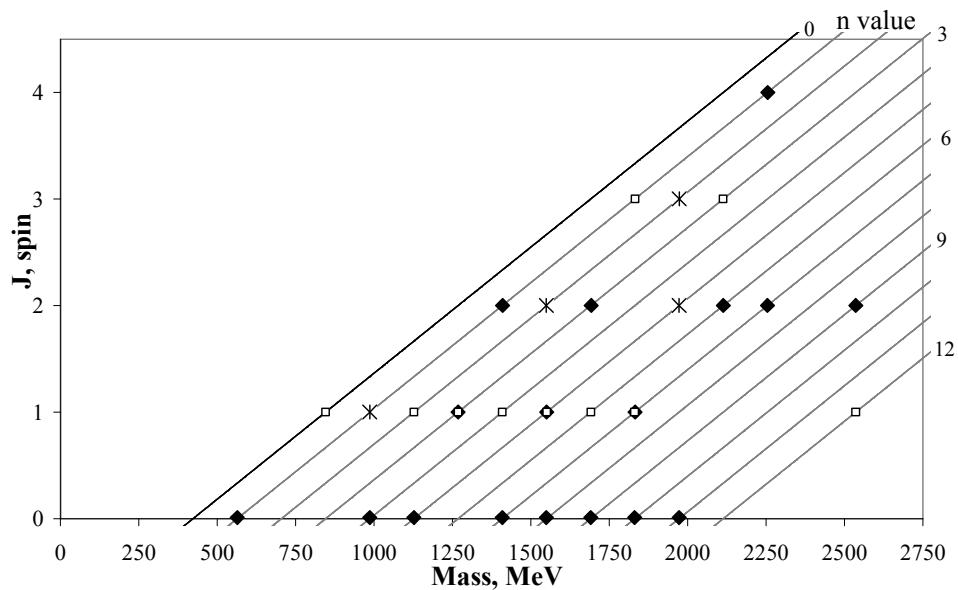


Fig.4.2 The theoretical relationship between spin and mass for light unflavoured mesons, assuming negligible binding energy between pearls of mass m_{μ}' according to Eq.(4.3). Several mesons coincide in mass. Four strange mesons (\mathcal{X}) have been added to fill vacancies but several positions remain vacant.

5. Strange mesons

5.1 General features

When angular momentum is plotted against mass for strange mesons, it is apparent that a linear relationship exists, even though many points are vacant, see Figure 5.1. A reasonable fit exists for the empirical formula:

$$M_K \approx 2.875(J + n/3)m_{\pi_0} + m_{K_{\pm}} \quad (5.1)$$

$$\approx m_{\pi_0}(3J + n)(1 - 1/24) + m_{K_{\pm}}$$

where n is an integer for the parallel lines as marked, and ($m_{\pi_0} = 134.9766\text{MeV}/c^2$), ($m_{K_{\pm}} = 493.677\text{MeV}$) are the pionet and kaon masses. This is like Eq.(4.1) and suggests that individual pionets are added to increment meson mass. The mean deviation of actual meson masses from Eq.(5.1) is $14\text{MeV}/c^2$, which is good compared with $32\text{MeV}/c^2$ for a theoretical random mass distribution.

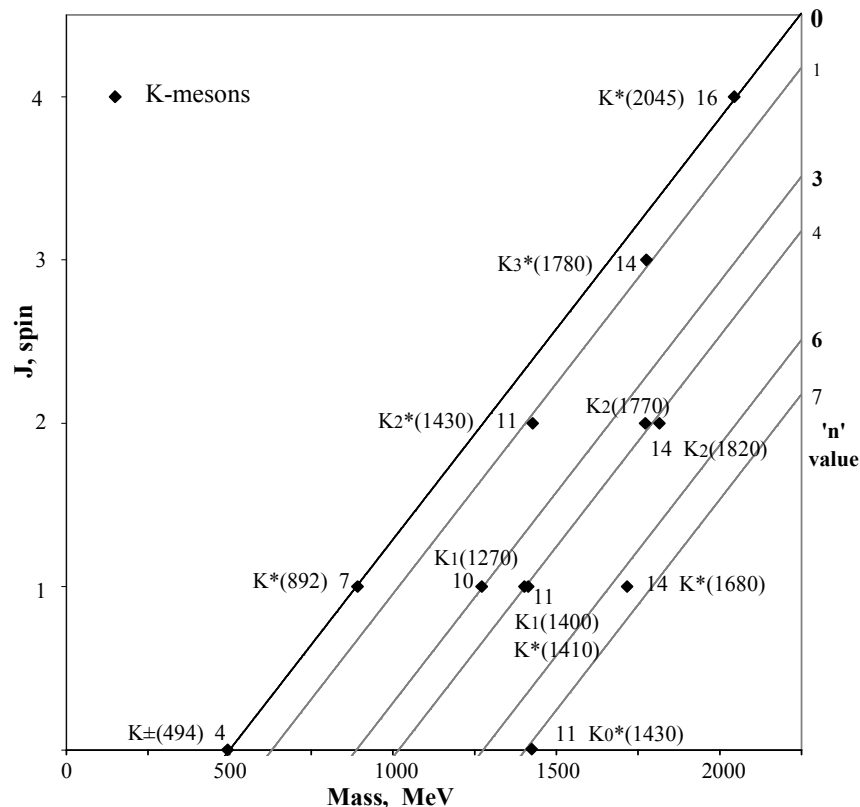


Fig.(5.1) A plot of strange meson spin against mass, according to Eq.(5.1) for the various values of 'n' given on the right ordinate. The number of pionets in each strange meson is marked.

Equation (5.1) implies that a strange meson resonance can easily decay into a *single* long-lived kaon plus pieces, albeit its own mean lifetime is very short. Likewise, an unflavoured meson such as $\phi(1020)$ can produce a $K\bar{K}$ pair when it has a quion and antiquion of sufficient mass.

Figure (5.2) represents our basic model for strange mesons, in which there are $(4 + n)$ neutral pionets bound by gluons in the compact core of radius r_{ok} . At charge radius r_{\pm} there is a positron for K^+ (matter) or an electron for K^- (antimatter). At the same radius there may also be a neutralising electron to produce a neutral kaon K^0 (matter), or neutralising positron to produce a neutral \bar{K}_L^0 (antimatter). It is this neutralising electron which is emitted during semi-leptonic decay of the K^0 , and vice-versa. These two neutral mesons are antiparticles and differ because the core pionets have right-handed helicity within the original K^+ or left-handed helicity within the original K^- , (just as a neutron differs from an anti-neutron).

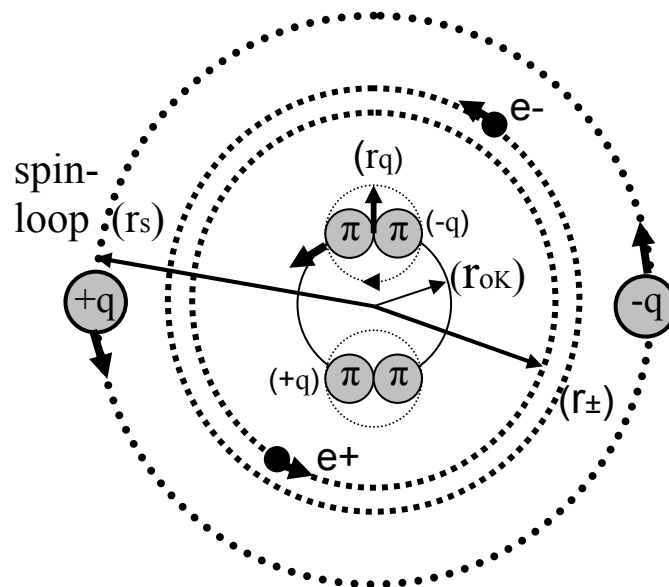


Fig.(5.2) Basic model schematic design for strange mesons, showing 4 pionets at the centre, orbited by a positron or electron, or both for a neutral meson. Pionets may also be added to the core to increase the value of n . Spin J is accomplished by adding pionets to the quion /antiquion pair in the spin-loop.

The core always has zero *net* spin, but overall meson spin may be produced by the quion /antiquion pair travelling in a larger spin-loop of radius r_s at velocity c . During hadronic decay, this spin-loop material plus n core pionets may convert rapidly into free π , ρ , etc., eventually leaving the central kaon ($2\pi^0 + 2\pi^0$) intact. This spin-loop may only exist for less than one rotation period, although its creation must have been completed more rapidly. For example, $K^*(892)$ has a decay full width ($\Gamma = 50.75$ MeV) which corresponds to a lifetime of ($\tau = \hbar/\Gamma = 1.3 \times 10^{-23}$ sec). Its spin-loop period is given by ($2\pi r_s / c = 2.12 \times 10^{-23}$ sec), according to Eq.(5.4). In the case of $K_4^*(2045)$, its lifetime is only 0.33×10^{-23} sec and its spin-loop period is also 2.12×10^{-23} sec. Consequently, strange mesons with spin hardly come into existence before decaying.

The spin of a strange meson is always given by:

$$J\hbar = (M_S / 2)cr_s \quad , \quad (5.2)$$

where M_S is the *quion+antiquion* mass travelling at velocity c around the spin-loop at radius r_s . Given Figure (5.1), we will arbitrarily let the n pionets reside in the core, so that 3 pionets must be added to the spin-loop to increase J by unity, then:

$$M_S \approx J \times 2.875m_{\pi_0} \quad , \quad (5.3a)$$

and Eq.(5.1) becomes:

$$M_K \approx M_S + \left[\left(\frac{2.875}{3} \right) nm_{\pi_0} + m_{K^\pm} \right] \quad . \quad (5.3b)$$

The spin-loop radius is independent of J at:

$$r_s \approx \left(\frac{2\hbar}{2.875m_{\pi_0}c} \right) = 1.017 \text{ fm} \quad . \quad (5.4)$$

For all values of J , pionets added to the spin-loop are bound by *approximately* the same energy decrement, since the coefficient 2.875 implies:

$$2.875m_{\pi_0} = 3(1 - 1/24)m_{\pi_0} \quad . \quad (5.5)$$

The mass decrement ($m_{\pi_0}/24$) is due mainly to the quion's or antiquion's self-binding strong force, plus their mutual electromagnetic attraction.

5.2 Kaon mass structure

Kaons are denoted *strange* because of their long lifetime, which implies strong binding of the component parts. Kaon mass m_{K^+} represents 4 strongly bound pionets through the formula:

$$m_{K^+} = 493.677 \text{MeV}/c^2 \approx 4 \left(1 - \frac{2}{24} \right) m_{\pi^0} , \quad (5.6)$$

where pionet mass is $134.9766 \text{MeV}/c^2$. Here, the negative term represents binding energy which keeps the pionets together by the strong force. The core radius r_{OK} will be given the classical value for 4 pionets arranged as a quion/antiquion pair like the pion design:

$$r_{OK} = 2 \times (e^2 / 4m_{\pi^0}c^2) = 5.334 \times 10^{-3} \text{ fm} . \quad (5.7a)$$

Then, by analogy with the electron and proton, the K^+ charge radius is proposed to be:

$$r_{\pm} = \alpha^{-1} r_{OK} / 2 = 0.3655 \text{ fm}, \quad (5.7b)$$

where ($\alpha = 1/137.036$) is the fine structure constant. And a neutralising electronic charge can be impressed into this same orbit to yield a neutral kaon K^0 of mass ($m_{K^0} = 497.614 \text{MeV}/c^2$).

Now we recall that for the neutron in Paper 1, the neutralising heavy-electron around the proton had a mass determined roughly by its radius:

$$m'_{he} = e^2 / (c^2 r_{he}) . \quad (5.8a)$$

Consequently, the mass of the neutralising electron here (at r_{\pm}) might be simply:

$$m'_- = e^2 / (c^2 r_{\pm}) = 7.71 m_e = 3.94 \text{ MeV}/c^2 , \quad (5.8b)$$

which would account for the measured difference in mass between a neutral and charged kaon:

$$m_{K^0} - m_{K^{\pm}} = 3.937 \pm 0.028 \text{ MeV}/c^2 . \quad (5.9)$$

In addition, according to the neutron theory, the neutralising electron is also bound and stabilised by its own self-interaction guidewave binding energy; see Paper 1, Eq.(10.2.2). Therefore, the analogous expression for the binding energy here would produce a heavy-electron of energy:

$$m_- c^2 = 9m_e c^2 - \frac{e^2}{(2\pi r_{\pm})} = 7.773 m_e c^2 = 3.97 \text{ MeV} . \quad (5.10)$$

This could take the form of 3 groups of 3 nominal electron masses; like 3 pearls in the 3 trineons of a proton.

The measured charge radius for the K^\pm is $\langle r \rangle = 0.560 \pm 0.031 \text{fm}$, see PDG (2010). This is an *effective* interaction size, to be compared with our real *source* size ($r_\pm = 0.3655 \text{fm}$). Likewise, the effective/measured size of K^0 is $\langle r^2 \rangle = -0.077 \pm 0.010 \text{fm}^2$, which implies that the negative and positive charges together at r_\pm interact differently with electrons in liquid hydrogen, so as to produce a net effective radius.

5.3 Mean lifetime

The long lifetime of a kaon will be attributed to the surrounding charge, with due regard to its particular spin orientation. The basic K^+ has a core structure ($2\pi^0 + 2\pi^0$) which has not been observed to exist by itself without its positron. Decay of a kaon occurs via the weak force, which is simply interpreted as repulsion due to direct natural jostling between constituent pionets in their tight orbits.

K^+ . The kaons K^\pm have a central core period of ($2\pi r_{0K} / c = 1.12 \times 10^{-25} \text{secs}$), so the number of periods in its mean life ($\tau_\pm = 1.2380 \times 10^{-8} \text{secs}$) is:

$$N_K = \tau_\pm / (2\pi r_{0K} / c) = 1.11 \times 10^{17} \quad . \quad (5.11a)$$

This very large ratio is reminiscent of the pion Eq.(2.19), then:

$$\ln(1.11 \times 10^{17}) \approx 4\pi^2 \quad (5.11b)$$

is probably to do with guidewave action and coherence length. For example, after differentiating this and multiplying through by ($e^2/c = 4m_{\pi 0} c r_{0K} / 2 = 2m_q c r_q / 2$), we get:

$$N_K \int_{2\pi r_{0K}}^{2\pi r_{0K}} \left(\frac{1}{2} \right) \left(\frac{(e/2)^2}{z'} \right) dt \approx \int_0^{2\pi} \left(\frac{m_q}{2} \right) c r_{0K} d\theta \quad . \quad (5.11c)$$

On the left, pearl charge is ($e/2$) and the integral represents potential energy action required to create the pearl travelling around the core. The right side represents kinetic energy action of a quion as it travels at velocity c during one core revolution $2\pi r_{0K}$.

K_L^0 . The extended lifetime of this kaon ($\tau_{0L} = 5.116 \times 10^{-8} \text{s}$) implies that the neutralising heavy-electron must interact constructively with the co-rotating core. This lifetime represents a number of periods for the heavy-electron at r_\pm :

$$N_{K_{0L}} = \tau_{0L} / (2\pi r_\pm / c) = 6.68 \times 10^{15} \quad . \quad (5.12a)$$

Again this ratio is interesting because of its interpretation in terms of a guidewave's coherence time and action, through the formula:

$$\ln(N_{\text{KOL}}) \approx \pi(137/12) \quad , \quad (5.12b)$$

which, after differentiating may be reduced with Eq.(5.7) to:

$$\left(\frac{1}{137}\right)^{N(2\pi r_{\pm})} \int_{2\pi r_{\pm}} \left(\frac{1}{2}\right) \frac{e^2}{z} dt = \left(\frac{1}{24}\right) \int_0^{2\pi} \left(\frac{m_q}{2}\right) c r_{\text{OK}} d\vartheta \quad . \quad (5.12c)$$

This expression accounts for the long lifetime by coordinating action in the neutralising heavy-electron and the core mechanism. On the left, the integral is potential energy action required to create the electron with its spiralling electromagnetic guidewave, which communicates continuously with the core to stabilise it. Weighting coefficient (1/137) records that the electron core consists of 137 pearls, (see Paper 2). The integral on the right is kinetic energy action for a quion running around the core, at radius r_{OK} . Coefficient (1/24) confirms there were 24 original pearl-seeds in each pionet.

\mathbf{K}_s^0 . The greatly reduced lifetime of this kaon ($\tau_{\text{os}} = 0.8956 \times 10^{-10}$ s) implies that the neutralising heavy-electron with the native positron are not very successful at stabilising a counter-rotating core. However, the core by itself would not exist at all, so some stabilisation must be occurring. The lifetime may again represent a number of core periods ($2\pi r_{\text{OK}}/c = 1.12 \times 10^{-25}$ secs):

$$N_{\text{KOS}} = \tau_{\text{os}} / (2\pi r_{\text{OK}} / c) = 8.01 \times 10^{14} \quad (5.13a)$$

This ratio may be interpreted in terms of guidewave action and coherence through the formula:

$$\ln(N_{\text{KOS}}) \approx 4\pi^2 (e_n / \pi) \quad , \quad (5.13b)$$

which after differentiating may be reduced to an expression like Eq.(5.11c):

$$\left(\frac{\pi}{e_n}\right)^{N_{\text{K}}(2\pi r_{\text{OK}})} \int_{2\pi r_{\text{OK}}} \left(\frac{1}{2}\right) \left(\frac{(e/2)^2}{z'}\right) dt \approx \int_0^{2\pi} \left(\frac{m_q}{2}\right) c r_{\text{OK}} d\theta \quad . \quad (5.13c)$$

On the left, pearl charge is (e/2) and the integral covers action required to create the pearl and stabilising guidewave travelling around a quion loop. Factor (π/e_n) implies the participation of gluons in the process. The right side represents kinetic action of a quion as it travels at velocity c during one core revolution $2\pi r_{\text{OK}}$. This expression

coordinates the heavy-electron and core mechanisms, to produce some stability of the core for a short while.

The fact that K_L^0 and K_S^0 are produced in equal quantity will be attributed to random orientation of the core spin relative to the angular momentum of orbiting charge. Energy difference of $3.491 \times 10^{-12} \text{ MeV}$ between the states is then comparable with the hyperfine splitting of interstellar hydrogen ($5.874 \times 10^{-12} \text{ MeV}$). The higher energy state K_L^0 is expected to be for parallel spins, which is evidently more stable. Regeneration of K_S^0 during interaction of K_L^0 with matter is understandable in terms of spin inversion. Earlier, the extended lifetime of the K_L^0 relative to that of K^\pm was proposed to be due to the stabilising effect of the neutralising charge on the co-rotating core, through the spiralling guidewaves. This is analogous to the charged pion being more stable than the neutral pion.

According to observations, neutral kaons K_L^0 oscillate between the matter and anti-matter state while propagating. In quark theory, this has been explained (see Perkins, 2000), as being due to a second-order weak interaction which also causes K_L^0 and K_S^0 particles to have the different masses mentioned above:

$$\Delta m = m_{KL} - m_{KS} = 3.491 \times 10^{-12} \text{ MeV} / c^2, \quad (5.14)$$

and the oscillation period is ($\tau_0 = h/\Delta mc^2 = 1.18786 \times 10^{-9} \text{ s}$). Herein, the K_L^0 and \bar{K}_L^0 must have equal status and such oscillations could be attributed to a change in *helicity of the core* from right-handed for K_L^0 to left-handed for \bar{K}_L^0 , maybe due to prompting from the orbiting charges. Figure (5.3) illustrates our model for the 4 possible particles. It is only anti-parallel spin of the core, not helicity, which causes the shorter lifetime for K_S^0 and \bar{K}_S^0 .

Clearly, all *mean* lifetimes must be determined by definite internal mechanisms and may actually be related. For example, the long lifetime of K_L^0 may be related to the above oscillation period through ($\tau_{0L}/\tau_0 \approx 137/\pi$). And for some reason, two other lifetimes (K_\pm and K_S^0) are in the ratio ($\tau_\pm/\tau_{0S} \approx 137$).

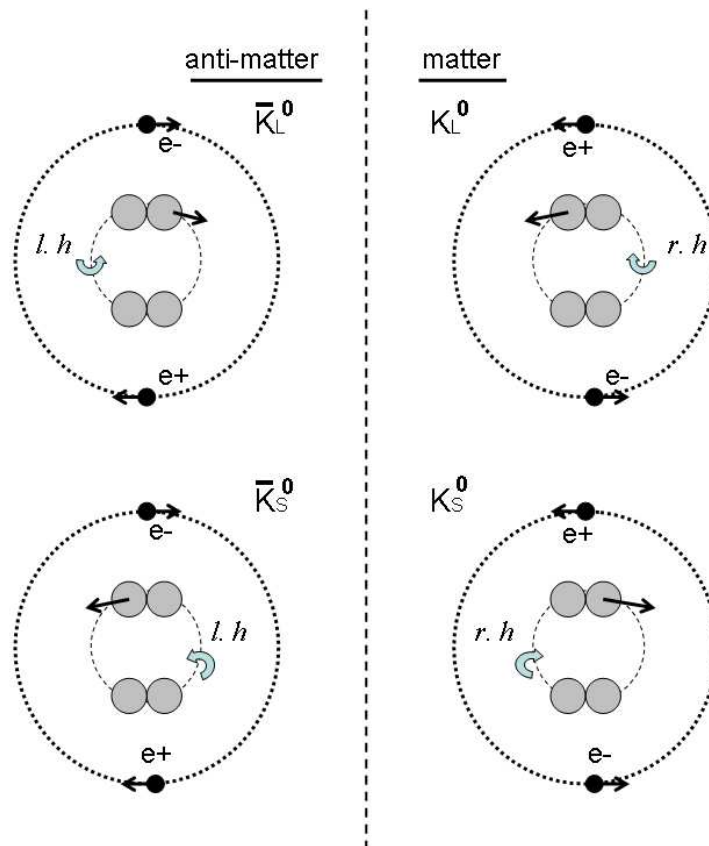
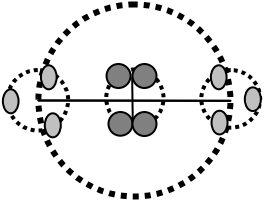
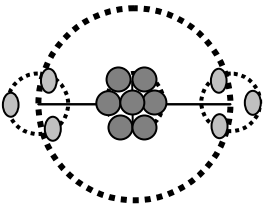
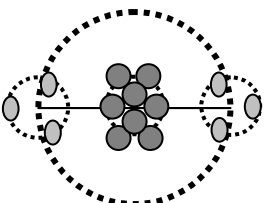
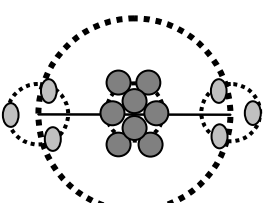
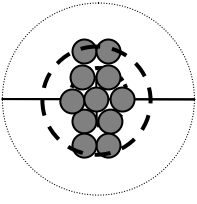
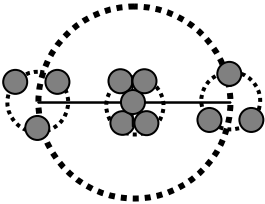


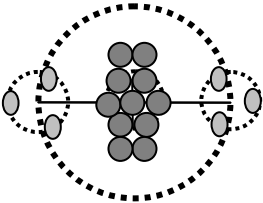
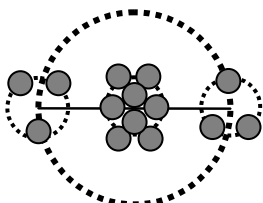
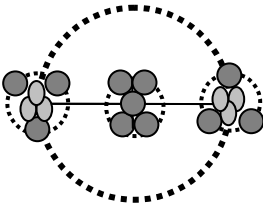
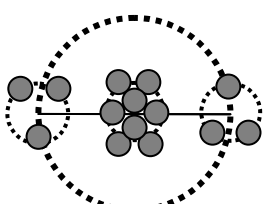
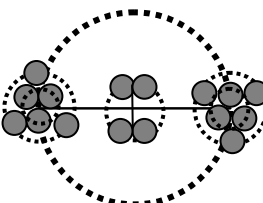
Fig.(5.3) Schematic diagram of the K_L^0 and K_S^0 neutral kaons with their anti-kaons \bar{K}_L^0 and \bar{K}_S^0 .

5.4 General designs

According to Figure 5.1 strange mesons consist of $(4 + n)$ bound pionets in a central core, plus a quion /antiquion pair in the spin-loop, as drawn in Figure 5.2. Three pionets must be added to the spin-loop to increase J by unity. By considering the decay products and kinetic energy, it is possible to derive a design for each one. Thus the decay process is to be regarded as relaxation, in which component parts separate ergonomically, preserving some features, especially when the free energy is low. Table 5.1 illustrates some simple tentative designs for strange mesons, and the formulae satisfy their mass distribution fairly well. The grey circles are pearls of pionet mass, and the small ovals have half the pionet mass.

Table 5.1 Tentative design of strange mesons, based upon ergonomic agreement with their decay products. The pearls shown as small ovals have half the pionet mass, only.

<p>7π</p> 	<p>K*(892) / 891.66 ± 0.26 MeV $\frac{1}{2}(1^-)$, $\Gamma = 50.8 \text{ MeV}$, Dy(K$\pi$) $m \approx 4m_{\pi_0} \left(1 - \frac{3/2}{24}\right) + 3m_{\pi_0} \left(1 - \frac{1}{24}\right)$ $= 894.2 \text{ MeV}$</p>
<p>10π</p> 	<p>K₁(1270) / 1272 ± 7 MeV $\frac{1}{2}(1^+)$, $\Gamma = 90 \text{ MeV}$, Dy(Kρ, K*(892)) $m \approx 7m_{\pi_0} \left(1 - \frac{3/2}{24}\right) + 3m_{\pi_0} \left(1 - \frac{1}{24}\right)$ $= 1273.9 \text{ MeV}$</p>
<p>11π</p> 	<p>K₁(1400) / 1403 ± 7 MeV $\frac{1}{2}(1^+)$, $\Gamma = 174 \text{ MeV}$, Dy(K*(892)π, Kρ) $m \approx 8m_{\pi_0} \left(1 - \frac{3/2}{24}\right) + 3m_{\pi_0} \left(1 - \frac{1}{24}\right)$ $= 1400.4 \text{ MeV}$</p>
<p>11π</p> 	<p>K*(1410) / 1414 ± 15 MeV $\frac{1}{2}(1^-)$, $\Gamma = 232 \text{ MeV}$, Dy(K*(892)π, Kρ) $m \approx 8m_{\pi_0} \left(1 - \frac{1}{24}\right) + 3m_{\pi_0} \left(1 - \frac{1}{24}\right)$ $= 1422.9 \text{ MeV}$</p>
<p>11π</p> 	<p>K₀*(1430) / 1425 ± 50 MeV $\frac{1}{2}(0^+)$, $\Gamma = 270 \text{ MeV}$, Dy(Kπ) $m \approx 11m_{\pi_0} \left(1 - \frac{1}{24}\right)$ $= 1422.9 \text{ MeV}$</p>
<p>11π</p> 	<p>K₂*(1430) / 1425.6 ± 1.5 MeV $\frac{1}{2}(2^+)$, $\Gamma = 98.5 \text{ MeV}$, Dy(K*(892), K$\rho$) $m \approx 5m_{\pi_0} \left(1 - \frac{1}{24}\right) + 6m_{\pi_0} \left(1 - \frac{1}{24}\right)$ $= 1422.9 \text{ MeV}$</p>

<p>14π</p> 	<p>K*(1680) / 1717 \pm 27 MeV $\frac{1}{2}(1^-)$, $\Gamma = 322$ MeV, Dy(Kπ, Kρ, K*(892)) $m \approx 11m_{\pi_0} \left(1 - \frac{2(3/2)}{24}\right) + 3m_{\pi_0} \left(1 - \frac{1}{24}\right)$ $= 1687.2\text{MeV}$</p>
<p>14π</p> 	<p>K₂(1770) / 1773 \pm 8 MeV $\frac{1}{2}(2^-)$, $\Gamma = 186\text{MeV}$, Dy(K₂*(1430), K*(892)) $m \approx 8m_{\pi_0} \left(1 - \frac{2}{24}\right) + 6m_{\pi_0} \left(1 - \frac{1}{24}\right)$ $= 1765.9\text{MeV}$</p>
<p>14π</p> 	<p>K₃*(1780) / 1776 \pm 7 MeV $\frac{1}{2}(3^-)$, $\Gamma = 159$ MeV, Dy(Kρ, K*(892)π, Kη) $m \approx 5m_{\pi_0} \left(1 - \frac{2}{24}\right) + 9m_{\pi_0} \left(1 - \frac{1}{24}\right)$ $= 1782.8\text{MeV}$</p>
<p>14π</p> 	<p>K₂(1820) / 1816 \pm 13 MeV $\frac{1}{2}(2^-)$, $\Gamma = 276\text{MeV}$, Dy(K₂*(1430), f₂(1270)) $m \approx 8m_{\pi_0} \left(1 - \frac{1}{24}\right) + 6m_{\pi_0} \left(1 - \frac{1}{24}\right)$ $= 1810.9\text{MeV}$</p>
<p>16π</p> 	<p>K₄*(2045) / 2045 \pm 9 MeV $\frac{1}{2}(4^+)$, $\Gamma = 198$ MeV, Dy(ϕK*(892), ρKπ) $m \approx 4m_{\pi_0} \left(1 - \frac{2}{24}\right) + 12m_{\pi_0} \left(1 - \frac{1}{24}\right)$ $= 2047.1\text{MeV}$</p>

Meson K₀*(1430) apparently has no net spin-loop yet accommodates 11 pionets. It has a very short lifetime ($\tau = 0.22 \times 10^{-23}$ s) and could consist of a quion + antiquion pair, which *closely* orbit the inner core of 7 pionets in counter-rotation.

5.5 Charge neutralisation of $K^*(892)$ and $K_2^*(1430)$

These two strange mesons have been measured in their neutral and charged states, well enough to analyze like the kaon:

$$K^*(892)^0 - K^*(892)^\pm = 4.28 \pm 0.34 \text{ MeV} \approx 8.38 m_e c^2 \quad , \quad (5.15)$$

$$K_2^*(1430)^0 - K_2^*(1430)^\pm = 6.8 \pm 2.0 \text{ MeV} \approx 13.3 m_e c^2 \quad . \quad (5.16)$$

As for the kaon, the increased mass of the neutralised meson will be attributed to adding a heavy-electron, without any change in the quion /anti-quion spin-loop or mass. In addition, an explanation of the particular heavy-electron mass value is desirable.

(a) $K^*(892)$. If, following Eq.(5.8a), the heavy-electron radius were smaller than the free electron radius at $r_{oe}/8.38 = 0.336 \text{ fm}$, it would be less than ($r_\pm = 0.3655 \text{ fm}$) in the central kaon. This could be an unstable orbit, in view of the earlier kaon analysis. Consequently, it is proposed that the heavy-electron is split into 3 loops of mass around $2.79 m_e$ each, but carrying only one electronic charge in total. The radius of this heavy-electron assembly is then $r_{he} \approx r_{oe} / 2.79 = 1.009 \text{ fm}$: just inside the quion /anti-quion orbit at 1.017 fm . If r_{he} is now substituted into Eq.(5.10) in place of r_\pm , then the resultant heavy-electron mass is ($m_c^2 \approx 8.56 m_e c^2 = 4.37 \text{ MeV}$), which is acceptable. It is thought that the heavy-electron actually travels around the spin-loop, with the gluons emitted by the quion and anti-quion. This extra mass would decrease the spin-loop radius slightly.

The compression sequence of the heavy-electron here follows that of the neutron, and by analogy in the final stage it is quantisable in terms of action because $[\ln(r_{oe}/r_{he}) \approx \ln(2.79) \approx \pi/3]$, which leads to an action integral by differentiating then multiplying by ($e^2 = m_e c r_{oe}$):

$$- \int_{2\pi r_{oe}}^{2\pi r_{he}} \frac{e^2}{z} dt \approx \frac{1}{3} \times \int_0^{2\pi} \frac{m_e}{2} c r_{oe} d\theta \quad . \quad (5.17)$$

On the left is the integral for potential energy action done in compressing the electron, and on the right is one third of the standard kinetic energy action of an electron core.

(b) $K_2^*(1430)$ The accuracy of this data is not enough for certainty but a model similar to $K^*(892)$ will be proposed with a heavy-electron mass of approximately

$14m_e$. If the heavy-electron radius were actually smaller than the free electron, at ($r_{he} \approx r_{oe} / 14 = 0.20\text{fm}$), it would be less than r_{\pm} in the central kaon. This is again unsatisfactory so let the heavy-electron be split into 5 loops of mass $2.8m_e$ each, but carrying only one electronic charge in total. The radius of this heavy-electron assembly is again coincidental with the spin-loop as for $K^*(892)$. It follows that the heavy-electron mass of 5 loops is around $(5/3)(4.37\text{MeV}/c^2) \approx 7.2\text{MeV}/c^2$. And the compression sequence of the heavy-electron follows that of the $K^*(892)$.

5.6 Mean lifetimes of K-mesons

(a) $K^*(892)$. The full widths of the charged and neutral mesons are similar, so their lifetimes are probably governed by their spin-loop or quion periods independent of the charge. The full width ($\Gamma_{K^*(892)} \sim 50 \text{ MeV}$) implies a lifetime ($\tau_K = 1.30 \times 10^{-23} \text{ s}$), which is less than the spin-loop period ($2\pi r_s / c = 2.13 \times 10^{-23} \text{ s}$ from Eq.(5.4)). It may instead be related to the period of the rotating quion ($2\pi r_q / c' = 1.55 \times 10^{-25} \text{ s}$):

$$N_{Kq} = \tau_K / (2\pi r_q / c') = 83.9 \quad , \quad (5.18)$$

and then,

$$\ln(N_{Kq}) = 4.43 = 0.448\pi^2 \quad . \quad (5.19)$$

Upon differentiating and multiplying by the general format [$e^2 / c = (2/\pi)^2 m_q c' r_q$], this reduces to an action integral like Eq.(3.2.8):

$$\int_{2\pi r_q}^{N_{Kq}(2\pi r_q)} \left(\frac{1}{2}\right) \frac{e^2}{z'} dt \approx \left(\frac{1}{2}\right) \int_0^{2\pi} \left(\frac{m_q}{2}\right) c' r_q \frac{d\theta}{3} \quad . \quad (5.20)$$

On the left is potential energy action required to create (or dissipate) a quion; where ($z' = c't$) over the guidewave coherence length. The integral on the right side represents kinetic energy action of a spinning quion over one third period ($2\pi r_q / 3$).

(b) $K_1^*(1270)$ through to $K_4^*(2045)$. The other K-mesons all have lifetimes less than $K^*(892)$, with their actions in the range 60% -100% of Eq.(5.20).

6. Conclusion

The quark/anti-quark singularity design of meson QCD theory has been replaced entirely by very well defined real particles. Particle mass represents

organised, localised energy, so the Higgs mechanism is not required. Detailed models of mesons have been derived in terms of structured components. First, pion design was derived by relating it to the muonic mass. A Yukawa potential was calculated for the hadronic field, analogous to the proton's field. By adding a heavy-electron or positron in a tight orbit around the hadronic core, a charged pion was produced. Other mesons were found to be ordered collections of muonnet or pionet masses, travelling in bound epicyclical orbits. Periods of these orbits were then related to the mean lifetimes of their mesons through specific action integrals. Decay products were descended from existing components within parent mesons, as expected for a relaxation process. This provided some traceability of particles and increased confidence in the analysis. The design of strange mesons with their relatively massive core was distinctly different from the flavourless mesons.

Appendix A: Compatibility with Standard Model

The models for an isolated proton, electron or muon given in Papers 1, 2, 3, were very successful at explaining the Yukawa potential, the reality of spin and anomalous magnetic moment, and particle creation mechanisms. On the other hand, the Standard Model of particle interactions has been very successful at accounting for data from high energy collision experiments. Consequently, the conceptual differences between these models can be explained if particles in collisions generate aspects not immediately apparent in static models. To link these models, the trineons in the proton and quions in mesons need to behave like up, down and strange quarks when in high energy collisions. It will be found that quark masses are specific for each particle type and not related necessarily to other particles. On average over many collisions, anti-quarks may even appear to be mixed with quarks in deep inelastic lepton-nucleon scattering experiments.

A.1 Proton and Neutron

Consider Figure A.1 wherein the proton of Paper 1 is depicted as 3 trineons travelling around the spin-loop at the velocity of light. Each trineon has a charge (+e) but only emits an electromagnetic field due to (+e/3) into the *exterior* space, so the proton's total external charge is (+e) as observed. Trineons also emit an e.m field *around* the spin-loop, equivalent to (+2e/3) each.

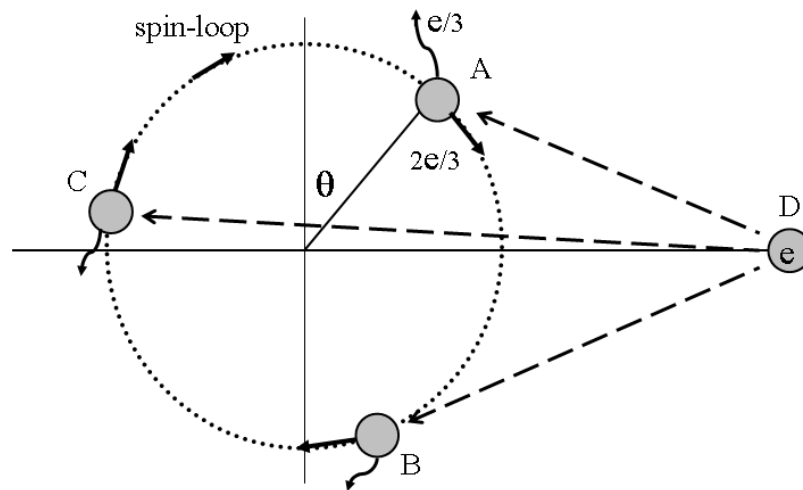


Fig.A.1 A schematic proton consisting of 3 trineons in the spin-loop with external and internal electromagnetic fields due to charge ($e/3$) and ($2e/3$), as experienced by an incident charge D.

Consequently, an energetic incident charge D is able to approach any one of the 3 trineons closely and will experience an interaction which depends upon the position and direction of that trineon within the spin-loop. For example, D on A will vary as $[e/3 + (2e/3)\cos(\theta)]$, whereas D on B will vary as $[e/3 + (2e/3)\cos(\theta+120^\circ)]$, and D on C will vary as $[e/3 + (2e/3)\cos(\theta+240^\circ)]$. These 3 possibilities for interaction of particle D with a proton are shown overlaid in Figure A.2. Clearly the effective interaction charge for a trineon can vary from $(3e/3)$ to $(-e/3)$.

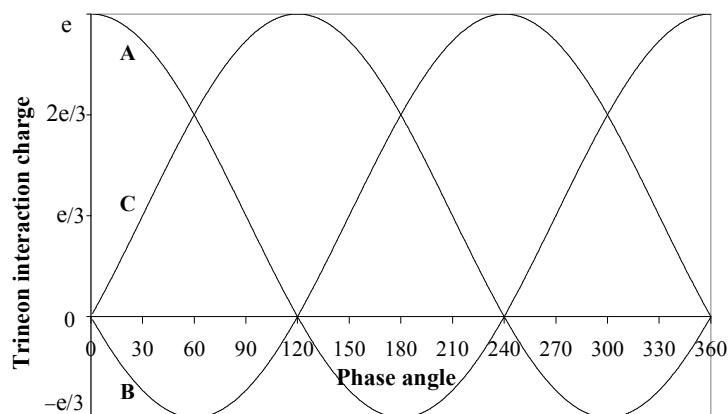


Fig.A.2 Variation of *interaction* charge for trineons A,B,C.

For correspondence with the Standard Model, we require $A(+2e/3)$, $B(-e/3)$, and $C(+2e/3)$, which occur at $(\theta = 60^\circ)$ where the squared values are nearest to each other: $A(4e^2/9)$, $B(e^2/9)$, $C(4e^2/9)$. It happens that the average of $[e/3 + (2e/3)\cos(\theta)]^2$ over one spin-loop cycle is $e^2/3$, which is also the average of quark charges-squared $(4e^2/9 + 4e^2/9 + e^2/9)/3$. The A,B,C, nominations are interchangeable at $(\theta = 120^\circ, 240^\circ)$.

Thus, the appearance of a negative *interaction* charge $(-e/3)$ within a positive proton is remarkable. This only happens for inelastic collision processes where a trineon reacts according to its internal mechanisms and direction of travel. Trineons are tightly confined by strong force gluons within a proton, so any collision of an incident particle with a single trineon might appear to involve a quark of spin-(1/2).

For the neutron model in Paper 1, a heavy-electron closely orbits the proton to neutralise its positive charge. Then if this heavy-electron joins with trineon A say, in opposing incident particle D, the effective interaction quark charges would be $A(-e/3)$, $B(-e/3)$, $C(2e/3)$ as required. This combining-process for a neutron as proposed will also be required for the meson interactions below.

A.2 Mesons

For the neutral pion model described in Section 2, the quion requires a total charge $(+e)$ according to creation equation (2.18). So, analogous to a proton's trineon, this charge appears to be distributed as $(+e/3)$ for an external field and $(+2e/3)$ for an internal field,. Consequently, a π^0 has the immediate appearance of a $d \tilde{d}$ quark pair. However, the quion with its internal charge $(+2e/3)$ is travelling around the meson circumference $(2\pi r_{\pi})$ at the velocity of light and could interact with an incident particle just like a trineon in the proton of Figure A.1. Thus, it could behave like an up or down quark, and the corresponding anti-quark could interact like an anti-up or anti-down quark. On average therefore, the π^0 can interact like a mixture of $u \tilde{d} \tilde{d}$ quarks.

The π^+ has an orbiting heavy-positron as in Figure 2.1. In a collision process, this positron combines with the anti-quion $(-e/3)$ to interact like an up quark, so the π^+ could be viewed as an $u \tilde{d}$ quark pair. Similarly, the π^- would interact like an $\tilde{u} d$ quark pair. Obviously, these meson quark assignments describe the charges only, and do not represent masses, which are less than in the proton. Masses of other unflavoured

mesons are multiples of the pionet mass, but their quion and anti-quion charges are the same as for the pions, as if this is the ground state.

Mesons with zero spin must generate spin for their quions as necessary during collisions, but mesons with spin can be considered to possess spin-1/2 quarks in collisions.

A.3 Strange quarks

Strange quarks were introduced to account for long lifetimes of some particles, and they also add more variety to the types of particles. In fact, the more massive strange particles decay *rapidly* into the long-lived lowest form, so that a strange quark does *not* extend the lifetime of its original particle. For example, heavy K-mesons described in Section 5 simply have a strongly-bound core which survives the initial rapid decay and converts to a kaon of long lifetime. Allocation of charge (-e/3) to a strange quark makes K^\pm analogous to π^\pm , and it also makes \bar{K}^0 the exact anti-particle of K^0 by way of helicity.

References

- Amendolia SR et al 1986 *Nucl Phys* **B277** 168-196
 Baru V et al 2003 *arXiv:hep-ph/0308129*
 Eschrich et al 2001 *Phys Lett* **B522** 233-239
 Gashi et al 2002 *Nucl Phys* **A699** 732-742
 Janssen G et al 1994 *arXiv:nucl-th/9411021*
 Parganlija D, Giacosa F, Rischke DH 2009 *arXiv:nucl-th/0911.3996*
 Perkins DH 2000 *Intro to High Energy Physics* 4th Ed Cambridge Univ Press
 Scadron MD et al 2003 *arXiv:hep-ph/0309109*
 Simo C 1978 *Celestial Mechanics* **18** 165-184
 Wang Z G & Yang W M 2005 *The European physical journal* **C42** 89-92
 Wayte R (Paper 1) 2010 A Model of the Proton www.vixra.org/abs/1008.0049
 Wayte R (Paper 2) 2010 A Model of the Electron www.vixra.org/abs/1007.0055
 Wayte R (Paper 3) 2010 A Model of the Muon www.vixra.org/abs/1008.0048